buildings

Article

Adaptive Optimization of Wind Environment in Coastal Village Spatial Forms of Western Guangdong

Yue Pang [1], Zhanxun Liang [1], Peisheng Xie [2] and Li Li [1,*]

[1] College of Architecture and Urban Planning, Guangzhou University, Guangzhou 510006, China; pangyue@gzhu.edu.cn (Y.P.); 2112209059@e.gzhu.edu.cn (Z.L.)
[2] Guangdong Provincial Architectural Design Research Institute Group Co., Ltd., Guangzhou 510000, China; xiepeisheng0419@outlook.com
* Correspondence: lili_ar@gzhu.edu.cn

Abstract: Naozhou Island is located in a subtropical marine monsoon climate, with frequent windy days throughout the year, which has a significant impact on the residents' lives. The spatial form of local traditional villages has adapted to the local wind environment through long-term practical exploration. This study aims to quantitatively analyze this layout to explore the patterns of its climate adaptability, thereby providing guidance for modern village construction. The research method primarily involves using CFD software (2019) to analyze the spatial form parameters of the village, namely village scale, planar form, building density, and orientation, along with their effects on average wind speed, wind speed amplification factor, and wind field coefficient under normal and extreme wind conditions. The results show that an appropriate planar form can enhance the wind adaptability of the village, while village scale and building density significantly affect the wind environment. However, the orientation of the village does not have a significant impact on wind field changes due to the discontinuity of the street system. These patterns of wind adaptability can assist in the planning and design of future coastal villages to enhance the wind environment regulation and disaster resilience of island villages.

Keywords: wind adaptation; coastal village planning; spatial morphology analysis; computational fluid dynamics (CFD); village microclimate; wind environment simulation

check for updates

Citation: Pang, Y.; Liang, Z.; Xie, P.; Li, L. Adaptive Optimization of Wind Environment in Coastal Village Spatial Forms of Western Guangdong. *Buildings* **2024**, *14*, 3721. https://doi.org/10.3390/buildings14123721

Academic Editor: Theodore Stathopoulos

Received: 29 October 2024
Revised: 16 November 2024
Accepted: 18 November 2024
Published: 22 November 2024

1. Introduction

Wind, as a natural phenomenon, plays an important role in multiple fields. From improving air quality [1] to alleviating the urban heat island effect [2], and to the fine design of vibration control in buildings or machinery [3], the influence of wind is ubiquitous. Particularly in island environments, wind not only shapes unique natural landscapes but also profoundly affects the living conditions and construction methods of local residents. Island inhabitants demonstrate a deep understanding and adaptability to the wind environment when faced with unique climatic conditions. This adaptability is particularly evident in architecture, manifested in low and less dense coastal village buildings, wide street dimensions, and other spatial forms that facilitate air circulation and reduce the hazards posed by extreme weather such as typhoons [4,5]. This wind adaptability not only reflects the harmonious coexistence of human wisdom and the natural environment but also provides valuable experience for modern architectural design.

Currently, research on the impact of spatial morphology on wind environments has made significant progress in urban areas [6–12], while studies in rural areas, especially coastal villages, remain relatively weak. Previous research on rural areas has mostly focused on landscape layout [13,14], village site selection, and feng shui theory [15,16], lacking in-depth exploration of the relationship between spatial morphology and wind adaptability. With the deepening implementation of the rural revitalization strategy, the living standards of villagers have significantly improved [17], and the sustainability of rural living environments has gained attention, making the demand for related research more urgent.

In existing research, many scholars have begun to focus on the relationship between the spatial morphology of inland villages and wind adaptability, achieving certain research results. For example, Xu et al. extracted the morphologies of 17 typical villages in Tianjin and used CFD to simulate the impact of different planar forms on village ventilation conditions and residents' health risks. Through statistical data analysis, they derived the optimal rural development morphology [18]. Zang et al. conducted quantitative analysis by selecting typical node spaces, considering the impact of village planar morphology and building density on wind speed, and proposed optimization and renovation suggestions to assist new village development [19]. Yao et al. explored how the location and spatial morphology of villages adapt to the local environment to promote the formation of a comfortable local microclimate [20]. Sun et al. used CFD to simulate and analyze the winter wind environment of four typical courtyard layouts, providing a theoretical basis for micro-level studies of village courtyard wind environments [21]. Gou et al. aimed to improve the energy efficiency of residential buildings in this region of China, exploring the relationship between spatial morphology and energy consumption in villages located in regions with hot summers and cold winters [22].

Scholars often use CFD numerical simulations and field measurements to explore the relationship between spatial morphological indicators such as building density, height, street orientation, aspect ratio, and village plan form with the wind environment [23–26]. However, most research subjects focus on inland villages under normal wind conditions, while studies related to island villages that are easily affected by typhoons remain a weak link. Considering the impact of wind on buildings under severe weather conditions is equally important.

The Pacific Northwest is the source of 36% of the world's typhoons [24]. According to publicly available data from the China Meteorological Administration, since 1949, a total of 264 typhoons have made landfall in Guangdong, occurring 277 times, ranking 1st in both the number of typhoons and landfall occurrences nationwide. Among the typhoons that made landfall in Guangdong, the Zhanjiang area is the most favored. During the peak typhoon season each year, residents of nearby islands, such as Naozhou Island, are troubled by these extreme weather events, making it a typical island affected by such climatic conditions.

Therefore, this paper takes the coastal village of Naozhou Island in western Guangdong as the research object, using CFD methods to analyze the impacts on the coastal village under two different wind conditions: normal wind and extreme wind. Through this study, we aim to reveal the patterns of how traditional layouts affect the wind environment, thereby providing a scientific basis for planners and architects to develop more effective strategies to enhance the wind adaptability of traditional villages. In addition, this research can also provide references for policy decision making and practical implementation in urban development, promoting sustainable and resilient design practices.

2. Materials and Methods

2.1. Research Subjects

Naozhou Island is an island located in the southeastern part of Zhanjiang City, Guangdong Province, formed approximately 200,000 to 500,000 years ago by underwater volcanic eruptions. It is also the largest volcanic island in China, bordered by Donghai Island to the north, Leizhou Bay to the west, and the South China Sea to the southeast, with a total area of about 56 square kilometers (Figure 1). Naozhou Island is situated in a subtropical monsoon zone, with prevailing easterly and southeasterly winds from April to September. From October to March of the following year, northerly and northeasterly winds dominate (Figure 2). Additionally, the island is often affected by typhoons to varying degrees during the summer. These typically occur from May to November, with the majority happening from July to September [27]. This results in two distinctly different states of wind conditions along the coastal areas throughout the year. One is a relatively stable and common state, known as the normal state; the other is an extreme and abnormal state, characterized by strong winds and heavy rainfall brought by typhoons and other extreme weather conditions.

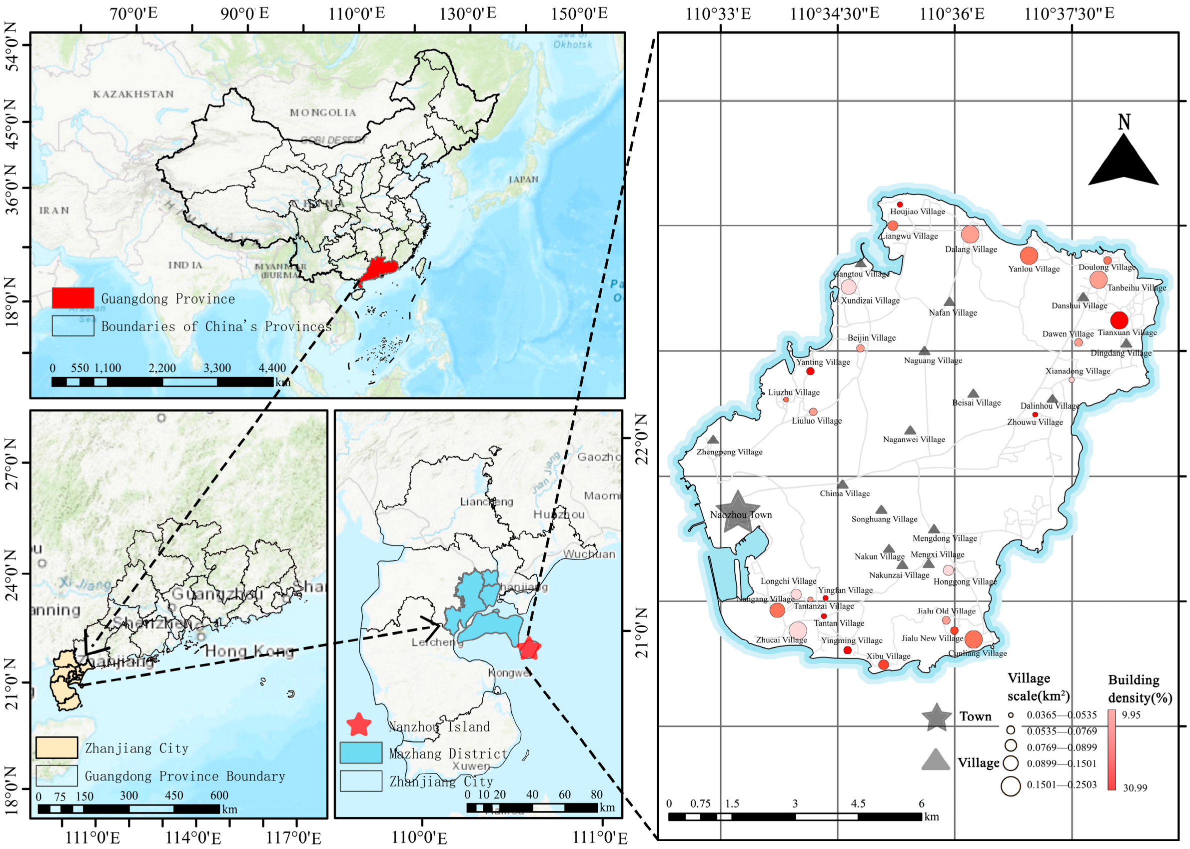

Figure 1. Location map of Naozhou Island.

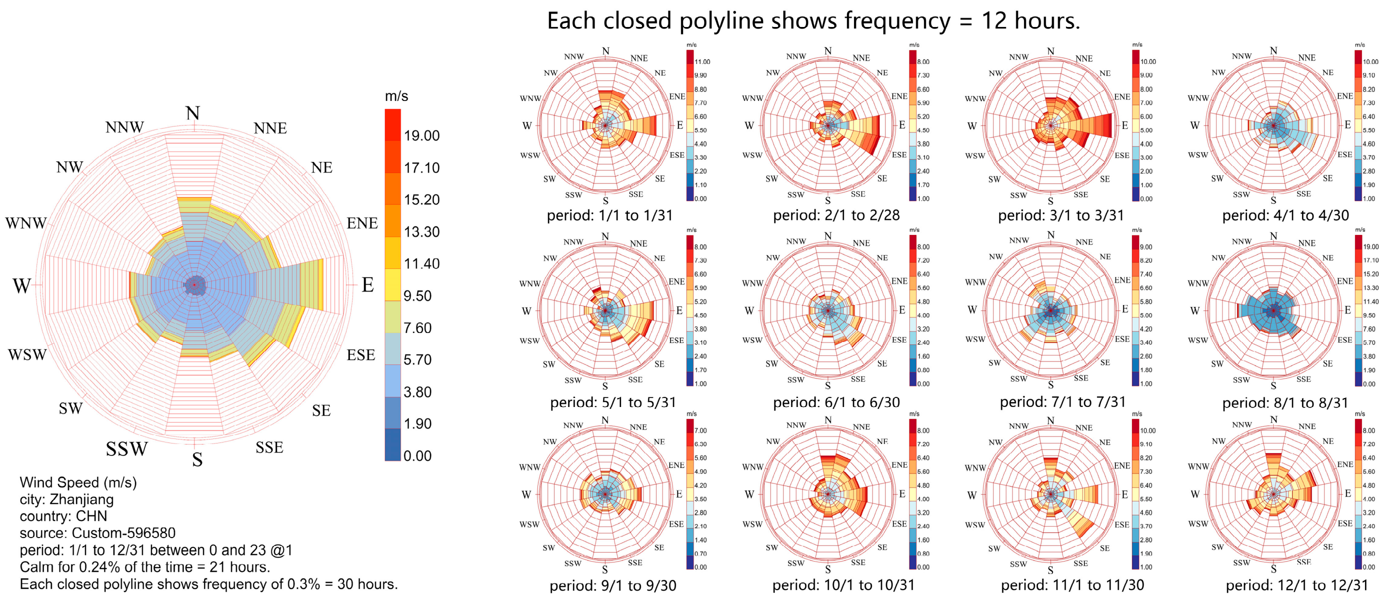

Figure 2. Climate map of Naozhou Island.

The research object of this paper focuses on 42 coastal natural villages on Naozhou Island that have a certain scale (with areas ranging from 0.01 km^2 to 0.26 km^2). The research content includes the spatial morphology of coastal villages on Naozhou Island, including village plan morphology, village scale, village orientation, and building density, providing a foundational basis for summarizing the regularity of spatial morphology indicators of coastal villages on Naozhou Island.

Characteristics of Village Spatial Morphology

- Village Spatial Morphology

Most villages on Naozhou Island exhibit a certain pattern in their planar forms. The coastal villages can be categorized into two types based on their planar layouts: compactly arranged collective villages and loosely arranged dispersed villages (Table 1).

Table 1. The planar morphology of the villages on Naozhou Island.

Village Morphology		**Simplified Schematic Diagram**	**Typical Village Planar Morphology**	**Feature Description**
Set class	Checkerboard layout	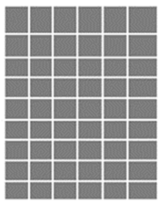	 CunLiang Village	The buildings are arranged neatly like chess pieces; the architectural layout is rigorous, with a strong sense of order, and the overall arrangement is compact.
	Clustered layout	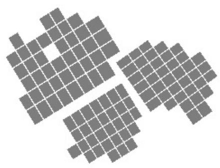	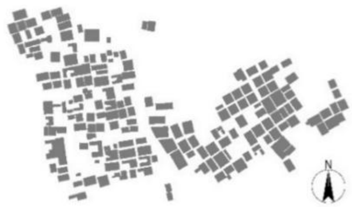 ZhuCai Village	Several clusters of habitation are separated by roads, woods, and ponds, yet are connected as a whole.
Dispersed Category	Strip layout	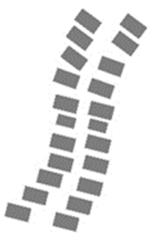	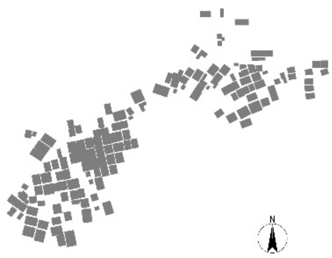 LongChi Village	Buildings are scattered along both sides of straight or curved roads, resulting in poor overall coherence.
	Scatter layout		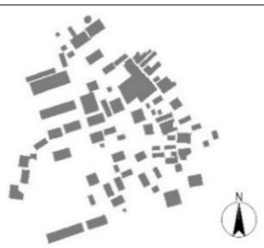 GangTou Village	The buildings have no fixed orientation and are flexibly distributed within the village at certain distances, resulting in a dispersed and unordered overall layout.

According to statistics (Table A1), the majority of coastal villages on Naozhou Island are clustered layout villages, with both grid layout villages and group layout villages numbering 16 each, accounting for 38.1%; in contrast, the dispersed layout includes strip layout villages and scattered layout villages, which represent a smaller proportion at 21.4% and 2.3%, respectively. The compact spatial layout demonstrates better wind resistance compared with the loose spatial layout, and grid layout villages and group layout villages are more compact than linear and scattered layouts, with a combined proportion of 76.2%. This is somewhat related to the frequent typhoon attacks on Naozhou Island, as a compact village spatial form can reduce the impact of typhoons to some extent.

- Village Scale

Based on field research and measurement data from Google Earth aerial images, the village scale is divided into five categories (Table 2). A statistical analysis of the village scales of 42 coastal villages on Naozhou Island (Table A1) reveals significant variations in scales among these villages. The smallest village is Dingdang Village, located on the eastern side of Naozhou Island, with an area of only 0.029 km^2; the largest village is Tianxuan Village, also on the eastern side of Naozhou Island, with a total area of 0.26 km^2. In terms of the proportional distribution of village scales, micro-scale villages (0.01–0.04 km^2) and super large-scale villages (greater than 0.2 km^2) account for a small proportion, both at 7.1%; large-scale villages (0.1–0.2 km^2) account for 16.7%; small-scale villages (0.04–0.1 km^2); and medium-scale villages (0.07–0.1 km^2) are the most common on Naozhou Island, each accounting for nearly one-third, at 38.0% and 31.0%, respectively.

Table 2. Statistical table of coastal villages of different scales on Naozhou Island.

Category	Aerial Photograph of a Typical Village	Typical Village Names
Micro-villages (0.01∼0.04 km^2)		Yingfan Village, Tantan Village, Dingdang Village.
Small villages (0.04∼0.07 km^2)		Zhouwu Village, Yingming Village, Dawen Village, Danshui Village, Houjiao Village, Yanting Village, Liuzhu Village, Mengxi Village, Naganwei Village, Tantanzai Village, Jialiu Old Village, Gangtou Village, Zhengpeng Village, Nakunzai Village, Xianadong Village, Liuluo Village.
Medium-sized village (0.07∼0.1 km^2)		Jialixin Village, Honggong Village, Doulong Village, Beijin Village, Chima Village, Songhuang Village, Nakun Village, Beizhai Village, Longchi Village, Xibu Village, Liangwu Village, Nafan Village, Naguang Village.

Table 2. *Cont.*

Category	Aerial Photograph of a Typical Village	Typical Village Names
Large villages (0.1∼0.2 km^2)		Cunliang Village, Dalang Village, Nangang Village, Xundizai Village, Tanbeihu Village, Yanlou Village, Dalinhou Village.
Super large village (greater than 0.2 km^2)		Zhucai Village, Tianxuan Village, Mengdong Village.

- Building Density

The overall terrain of Naozhou Island is flat, and the populations in the villages are relatively small, providing ample space for construction and public areas within the villages. At the same time, the lower building density in the villages not only contributes to good ventilation but also serves as an intuitive reflection of the relatively dispersed spatial layout of the various villages on Naozhou Island. According to statistical results (Table A1), the building density of coastal villages on Naozhou Island is low, generally not exceeding 50%. Villages with building densities of 10% to 20% and 20% to 30% account for the largest proportions, comprising 38% and 50% of all villages, respectively; there are 2 villages each with building densities of 10% and 30% to 40%, each accounting for 5%; and among the 42 villages, only 1 village has a building density exceeding 40%. These factors collectively contribute to the characteristic low building density of the villages on Naozhou Island.

- Orientation of the Village

Combining field research with Google Earth aerial images, a statistical analysis of the orientations of 42 coastal villages on Naozhou Island was conducted (Table A1). The results show a clear pattern in village orientations: the most common orientations are north–south and northwest–southeast, each accounting for 28.6%, together comprising nearly two-thirds of the villages. Other orientations have a lower proportion, and, additionally, 4.7% of the villages have unclear orientations. The formation of this orientation distribution is closely related to the unique natural environment and climatic conditions of Naozhou Island. The island experiences prevailing south and southeast winds throughout the year; to adapt to this wind pattern, most villages have chosen north–south or southeast orientations to maximize the use of natural wind power and enhance internal ventilation. At the same time, Naozhou Island enjoys a warm and humid climate with ample sunlight. These climatic conditions allow village orientations to be flexible rather than strictly adhering to the traditional north–south principle, enabling adjustments based on actual needs and topographical features, thus resulting in diverse orientation characteristics. Further analysis reveals that villages close to the coastline, such as Yingming Village and Xibu Village in the south of the island, tend to face the sea, while villages in the north, like Yanlou Village, choose a northern orientation based on topography and wind direction. The orientation of these villages towards the sea serves both ventilation purposes and is related to local customs, such as the construction of Mazu temples facing the sea to pray for the safe return of family members who go out to sea.

2.2. Construction of the Wind Environment Evaluation System for Naozhou Island

Due to Naozhou Island's location in a subtropical monsoon climate region, the effects of humidity and heat are quite pronounced, along with 3 to 4 typhoons occurring each year, which pose a serious threat to the safety of the island's residents. Therefore, this study primarily evaluates the comfort and safety at a height of 1.5 m, corresponding to pedestrian level.

2.2.1. Classification of Wind Speed Levels on Naozhou Island

The existing literature [28] has proposed a classification standard for horizontal wind speed levels at a height of 1.5 m for outdoor pedestrian comfort in Hong Kong during the summer, specifically as follows: stagnant wind (V < 0.3 m/s), poor (0.3 m/s ≤ V < 0.6 m/s), low (0.6 m/s ≤ V < 1.0 m/s), generally acceptable (1.0 m/s ≤ V < 1.3 m/s), and good (V ≥ 1.3 m/s). Given that both Zhanjiang and Hong Kong belong to the subtropical climate zone, the two regions exhibit a high degree of similarity in climatic characteristics during the summer, both showing high temperatures and humidity. Additionally, according to historical meteorological data, the average summer temperatures in Zhanjiang and Hong Kong are 28.3 °C and 28.2 °C, respectively, with summer relative humidity at 82.2% and 81.9%. Therefore, this wind speed classification standard has a high degree of applicability for evaluating the wind speed values in the outdoor wind environment of Naozhou Island in Zhanjiang during the summer.

The summer gust wind speed on Naozhou Island ranges from 4.0 to 6.0 m/s, and the unpaved land in the villages is prone to dust raising. According to the "Technical Specifications for the Prevention and Control of Urban Dust Pollution"[29], wind speeds above level 4 (with a surface roughness $\alpha = 0.12$ converted to 4.4∼6.3 m/s) require dust prevention measures. This paper sets 4.4 m/s as the dust threshold. Additionally, combined with related studies, 5 m/s is defined as the critical value for wind comfort. Beaufort scale level 6 (approximately 8.6 m/s at pedestrian height) and level 7 (approximately 11.0 m/s) significantly affect outdoor activities. This paper refines the assessment of wind speed levels on Naozhou Island in summer and establishes a wind speed evaluation standard for the wind environment at pedestrian height (1.5 m), categorizing wind comfort into five levels (Table 3).

Table 3. Evaluation standards for wind speed values in the wind environment at 1.5 m above ground level on Naozhou Island in summer.

Wind Comfort Level	Wind Speed Grade	Pedestrian Height (1.5 m) Wind Speed	Pedestrian Perception	Remarks
Level 1: unsatisfied, the environment is stuffy and hot	1	V < 0.3 m/s	Calm wind, poor thermal comfort	Measures such as adding ventilation facilities or adjusting the landscaping layout should be taken to improve thermal comfort.
	2	0.3 m/s ≤ V < 0.6 m/s	Poor thermal comfort	
	3	0.6 m/s ≤ V < 1.0 m/s	Lower thermal comfort	Under the shelter of tree shade or building shadows, solar radiation is reduced, making this discomfort somewhat acceptable.
Level 2: satisfied, can engage in outdoor activities freely	4	1.0 m/s ≤ V < 1.3 m/s	Basic satisfaction with thermal comfort	Wind energy effectively alleviates heat and enhances human comfort.
	5	1.3 m/s ≤ V < 4.4 m/s	Better thermal comfort, without generating dust	

Table 3. *Cont.*

Wind Comfort Level	Wind Speed Grade	Pedestrian Height (1.5 m) Wind Speed	Pedestrian Perception	Remarks
Level 3: discomfort, outdoor activities slightly affected	6	4.4 m/s ≤ V < 5 m/s	Normal activities are affected, resulting in dust generation	The comfort of pedestrians decreases, and outdoor activities may be somewhat restricted; at this time, effective dust control measures should be implemented.
	7	5.0 m/s ≤ V < 8.6 m/s	Can be tolerated, normal activities are affected, resulting in dust generation	
Level 4: danger, outdoor activities severely affected	8	8.6 m/s ≤ V < 11.0 m/s	Discomfort severely affects normal activities and may pose a danger	Windproof reinforcement measures must be taken to ensure pedestrian safety and prevent accidents.
	9	11.0 m/s ≤ V < 13.6 m/s	Extremely uncomfortable, severely affecting normal activities, and potentially causing danger	
Level 5: dangerous, not suitable for outdoor activities	10	13.6 m/s ≤ V	The wind environment is severe and unbearable, which may pose a danger	The area is considered extremely unsafe and pedestrian access should be avoided as much as possible, with warning signs and protective measures in place.

2.2.2. Evaluation System for the Wind Environment of Naozhou Island

For the evaluation of the outdoor wind environment, common indicators include average wind speed, wind speed amplification factor, ratio of comfortable wind area, ratio of calm wind area, and ratio of strong wind area, among others. Definitions are provided below:

1. Average wind speed: the average wind speed at a height of 1.5 m for pedestrians at various points within the assessment area, used to evaluate the overall wind speed magnitude in the region.
2. Wind speed amplification factor: The wind speed amplification factor reflects the amplification effect of a building on wind speed, typically referring to the ratio of the maximum wind speed at a height of 1.5 m above the ground around the building to the wind speed at the same height in an open area. The calculation of the wind speed amplification factor can be performed using the following exponential function that describes the variation of average wind speed with height, this is example 1 of an equation [30,31]:

$$\begin{cases} v' = \frac{v_{1.5B}}{v_{1.5f}} \\ v_{1.5f} = v_{10f}\left(\frac{1.5}{10}\right)^{\alpha} \end{cases} \quad (1)$$

   v'—wind speed amplification factor. $v_{1.5B}$ —maximum wind speed at a height of 1.5 m above the ground around the building, $v_{1.5f}$ —wind speed at a height of 1.5 m above the ground in an open area away from the building, v_{10f}—wind speed at a height of 10 m above the ground in an open area away from the building, α—ground roughness index.
3. Comfortable wind zone area ratio: This assesses the ratio of the area of the comfortable wind zone at a height of 1.5 m for pedestrians to the total area of the outdoor open space. A larger comfortable wind zone area ratio (not exceeding 100%) indicates better wind environment quality of the site. In this paper, the wind speed value for the comfortable wind zone is taken as 1.0 m/s to 4.4 m/s.

4. Static wind area ratio: The ratio of the area of the static wind zone at a height of 1.5 m for pedestrians to the total area of outdoor open space within the assessment area. In this paper, the area where wind speed is less than 1 m/s at a height of 1.5 m for pedestrians is defined as the static wind zone. Under summer humid and hot climate conditions, the static wind zone can create a feeling of stuffiness, reducing comfort. A larger static wind area ratio indicates poorer ventilation in the assessment site and lower comfort levels.
5. Strong wind area ratio: The ratio of the area occupied by strong wind zones at a height of 1.5 m for pedestrians to the total area of open space within the assessment area. In this paper, areas where wind speeds exceed 5 m/s at a height of 1.5 m for pedestrians are defined as strong wind zones. Under summer humid and hot climatic conditions, while strong wind zones can dissipate heat, they also generate dust, making outdoor activities uncomfortable and potentially leading to safety issues. The larger the area of strong wind zones, the poorer the wind comfort.

In assessing the wind environment quality of coastal villages on Naozhou Island, this paper employs various indicators that have been widely used in this field [5,32,33]. However, to more comprehensively reflect the characteristics of the village's wind environment under different wind conditions, this article will utilize two wind field coefficients, K1 and K2.

6 The setting of K1 is designed to assess the ventilation efficiency and comfort of the site by comparing the ratio of the area of comfortable wind zones to that of stagnant wind zones under normal wind conditions. This can intuitively reflect the proportion of comfortable wind environments in the village and the proportion of poorly ventilated areas under normal wind conditions, thereby providing us with a basis for improving and optimizing the wind environment.

7 The setting of K2 is designed to address challenges under extreme wind conditions. In extreme wind conditions, the emergence of strong wind zones can significantly reduce the wind comfort of the site and may even pose a threat to the lives and safety of residents. Therefore, by comparing the ratio of the area of comfortable wind zones to the area of strong wind zones, we introduce the coefficient K2 to assess the wind resistance capability and the stability of the wind environment of the site under extreme wind conditions. A larger value of K2 indicates that the site can still maintain good wind comfort under extreme wind conditions, which is of great significance for improving the quality of life and safety of residents.

From the above, it can be seen that the average wind speed, as a fundamental and intuitive indicator, can reflect the overall wind speed level within the assessment area, helping to understand the basic characteristics of the wind environment in the village. The wind speed amplification factor is used to quantify the amplification effect of wind speed in specific areas, which is significant for assessing regions within the village that may experience excessively high local wind speeds. The K1 and K2 coefficients combine three indicators—the area ratios of comfortable wind zones, calm wind zones, and strong wind zones—to obtain ventilation efficiency and comfort under different wind conditions (normal and extreme). Together, they reflect the basic characteristics of the wind environment, local amplification effects, and comfort and stability under varying wind conditions. In summary, this paper conducts a comprehensive evaluation of the wind environment in coastal villages on Naozhou Island using four indicators: average wind speed, wind speed amplification factor, wind field coefficient K1, and wind field coefficient K2.

2.3. Research Methods

This study comprehensively employs both field measurements and numerical simulations to assess the wind environment quality of the villages on Naozhou Island. First, field measurements are conducted in selected typical villages to understand their wind environment characteristics. These measured data are used not only to evaluate the current wind environment quality but also as a key basis for verifying the accuracy of PHOENICS simulations. Subsequently, the PHOENICS software (2019) is used to simulate the wind field at pedestrian height in the village under different spatial morphology indicators, calculating relevant parameters of a single spatial index variation model to conduct an in-depth analysis of the village's wind conditions, and providing a scientific basis for improving wind environment quality.

2.3.1. Measured Wind Environment

To clarify the wind environment characteristics of the coastal villages on Naozhou Island, this paper selected Yingming Village, which has the highest proportion of the four morphological indicators previously mentioned, for field research. Wind environment-related measurements and analyses were conducted (Figure 3). During the measurement process, a total of 10 measurement points were arranged to comprehensively and accurately capture the overall wind environment of Yingming Village, ensuring the completeness and accuracy of the data. The Kestrel 500 weather station was used to measure the wind environment in the streets and alleys of Yingming Village, along with the wind environment at the village boundary. The measurement time selected was the period from 9:00 to 20:00 on a typical summer day (15 July 2022).

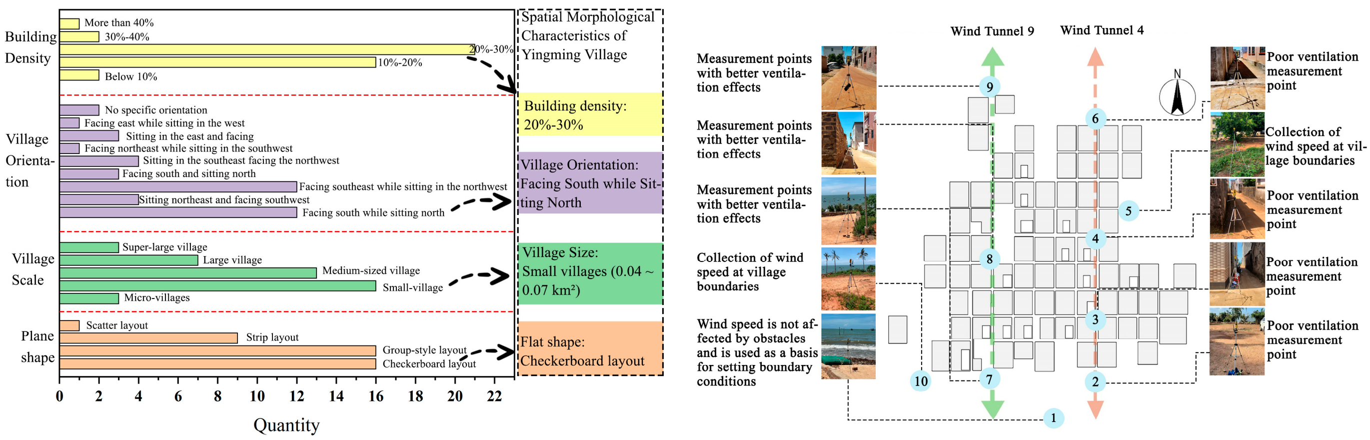

(**a**) (**b**)

Figure 3. Typical selection and measurement point layout of Yingming Village. (**a**) Typical village selection; (**b**) measurement point distribution map.

2.3.2. Analysis of Measured Results

- Analysis of Wind Sources

From Figure 4, it can be seen that between 8:00 and 20:00, the wind field in Yingming Village exhibits multiple regular fluctuations of "rise/fall." Taking measurement points 1 and 10 as examples, both points are direct wind sources from the southern seaside, and their wind speed and direction throughout the day are relatively close. Measurement point 1 is closest to the seaside, with no plants or structures obstructing it. The average wind speed at measurement point 1 throughout the day is 3.3 m/s, with a maximum wind speed of 4.6 m/s, and the predominant wind direction is southeast. In the morning, the wind speed is relatively stable, averaging 3.0 m/s, while, in the afternoon, the wind speed increases and varies significantly. The average wind speed at measurement point 10 throughout the day is 2.8 m/s, with the main wind direction being south and a maximum wind speed of 4.5 m/s. The wind speed in the morning is relatively stable, but in the afternoon, influenced by surrounding vegetation, the fluctuations in wind speed and direction at measurement point 10 are more pronounced compared with measurement point 1.

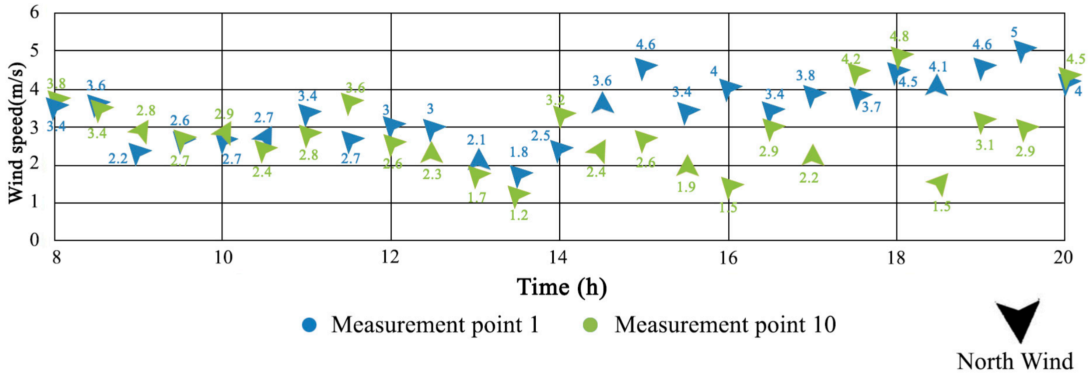

Figure 4. Measurement point 1 and measurement point 10 wind speed and wind direction.

- Wind Channel Analysis

According to the measured results, the wind environment speed in Yingming Village is influenced by internal and external obstacles within the village and the wind pressure of the wind field. The wind speed gradually decreases from south to north, while the wind direction remains relatively constant. Taking the measured results at 8:00 as an example, the wind speed in wind channel 4 (with measurement points 2, 3, 4, and 6) decreases from 2.6 m/s at measurement point 1 to 0.0 m/s at measurement point 6 (Figure 5). In wind channel 9 (with measurement points 7, 8, and 9), the wind speed decreases from 3.1 m/s to 1.3 m/s, and the trend of decreasing wind speed from south to north in wind channel 9 is more pronounced. It can be observed that from 8:00 to 20:00, the wind speed at measurement point 7 is greater than that at measurement point 9 for most of the time.

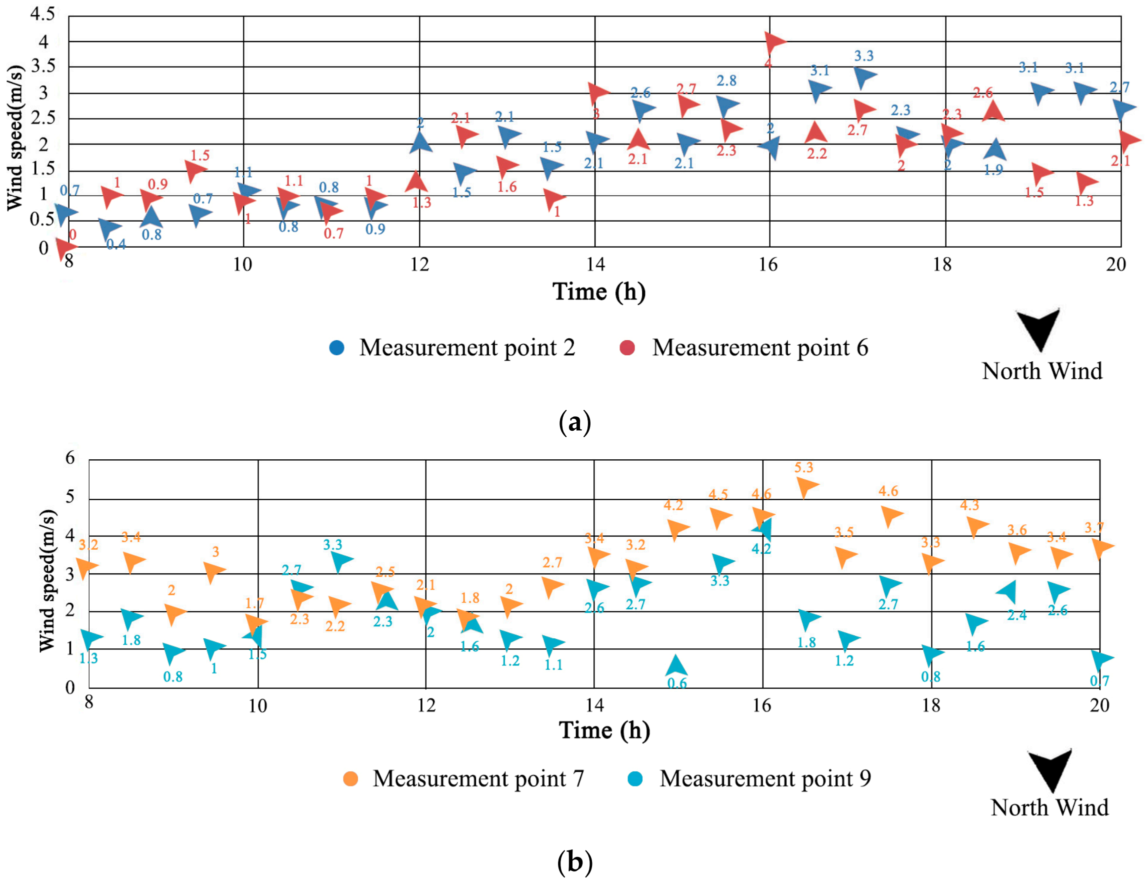

Figure 5. Wind speed and direction at measurement points of two wind channels: (**a**) wind channel 4; (**b**) wind channel 9.

Through the measurement of the wind environment on typical summer meteorological days in Yingming Village, the following characteristics can be observed: the overall wind speed in Yingming Village on typical summer meteorological days is relatively low and varies little, with an average wind speed below 3.0 m/s. The wind direction is also quite stable, predominantly from the southeast, with occasional south winds; the incoming wind is weakened by the village, and, after passing through the village, there is a noticeable attenuation in wind speed.

2.3.3. Software Simulation and Verification

- Simulation Verification

Numerical simulation based on computational fluid dynamics (CFD) is one of the important tools for improving urban wind environments [34,35]. The most common CFD methods include two types: Reynolds-averaged Navier–Stokes (RANS) and large eddy simulation (LES). RANS is known for its cost-effectiveness and reasonable accuracy in various turbulent flows, as it directly solves the mean flow and simulates turbulence across all scales [36]. RANS-based CFD software includes PHOENICS, Fluent, COMSOL, etc. Due to PHOENICS' strong openness, ease of use, and suitability for industrial applications and scientific research, it has been widely used [37]. Whether for small-scale village buildings or large-scale residential areas, the error between measurement results and simulation results is within an acceptable range (less than 10%). Therefore, the use of PHOENICS software for wind environment simulation has good reliability [4,38]. This paper uses PHOENICS for the wind environment simulation of Niao Island (Figure 6), with the initial parameters and boundary conditions for the simulation as follows:

- Grid accuracy setting: the manual setting is used to ensure that each grid cell is less than 4 m, with a grid gradient rate of 1.2 applied.
- Wind environmental boundary conditions: based on the survey, the normal wind condition is set as a southeast wind with a wind speed of 2.57 m/s; the extreme wind condition is set as an east wind with a wind speed of 21.70 m/s according to meteorological station data.
- Number of iterations: 3000 iterations are completed to ensure the stability of the results.
- Surface roughness index is set at 0.12, reflecting the impact of surface characteristics on the wind field.

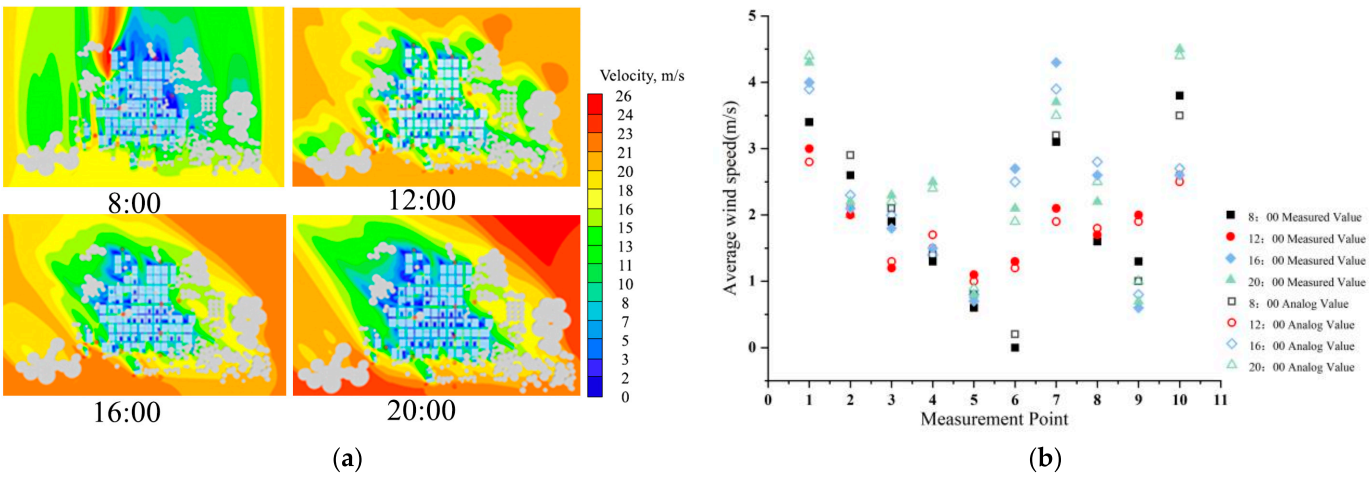

Figure 6. Measured and simulated analysis of Yingming Village. (**a**) Simulated wind speed cloud map at four moments; (**b**) comparison of simulated wind environment values and measured values.

Through the comparative analysis of the simulated values and the measured values at 10 measurement points (Figure 6), it can be observed that the trends in wind speed and direction for the 10 measurement points are consistent between the simulated and measured values. During the same time period, the trends of rising or falling wind speed are essentially the same for both measured and simulated data. Overall, the measured values and simulated values at the 10 measurement points at 4 different times do not differ significantly, with a difference of 0 to 0.3 m/s, and the measured wind direction is generally consistent with the simulated wind direction.

- Goodness-of-Fit Analysis

The goodness of fit refers to the degree of agreement between the model's predicted results and the actual values. Here, it is used to examine the degree of agreement between the simulated wind speed results and the measured values. Common testing methods include residual sum of squares test, chi-squared test, linear regression test, etc.

This paper uses the residual sum of squares for testing, This is example 2 of an equation:

$$Q = \sum (y - y^*)^2 \quad (2)$$

where y represents the measured value; y* represents the simulated value.

The goodness-of-fit index equation is given in (3):

$$R^2 = 1 - Q \quad (3)$$

The average fitting degree of the 10 measurement points at 8:00 is R^2 (8:00) = 0.67, at 12:00 is R^2 (12:00) = 0.78, at 16:00 is R^2 (16:00) = 0.67, and at 20:00 is R^2 (20:00) = 0.62.

The goodness of fit is averaged for the four time points as follows (4):

$$R^2_{Average} = (R^2_{(8:00)} + R^2_{(12:00)} + R^2_{(16:00)} + R^2_{(20:00)} \Big) / 4 = 0.685 \quad (4)$$

A goodness-of-fit value greater than 0.5 indicates that the fit is reliable. The fitting values for the 10 measurement points across 4 time periods are all greater than 0.6, with an average of 0.685, which is close to 0.7, indicating a high degree of agreement between the simulated and measured values. This suggests that the software can accurately describe the wind environment of a Naozhou Island village.

2.3.4. Model Establishment Based on Single Spatial Index Variation

To accurately analyze the wind environment characteristics of the villages on Naozhou Island, 27 villages with clear planning and uniform building orientations were selected from a total of 42 villages for in-depth discussion (Table A2). In contrast, scattered layout villages, due to their lack of fixed orientations and flexible distribution within a certain distance, exhibited a disordered and discrete overall pattern, which significantly increased the complexity and difficulty of wind environment simulation. Therefore, in this study of the wind environment simulation of coastal villages on Naozhou Island, scattered layout villages were not included in the analysis. Additionally, based on the results of field investigations of the spatial forms of the selected villages, we constructed four sets of models in the software simulation. In the model settings, the height of the buildings and the spacing between buildings were kept constant at 10 m (Figure 7). By adjusting the spatial form index values of each model group, we analyzed the changes in the village wind environment under different spatial form index values and two wind conditions (the normal wind condition being a southeast wind at a speed of 2.57 m/s; the extreme wind condition being an east wind at a speed of 21.70 m/s).

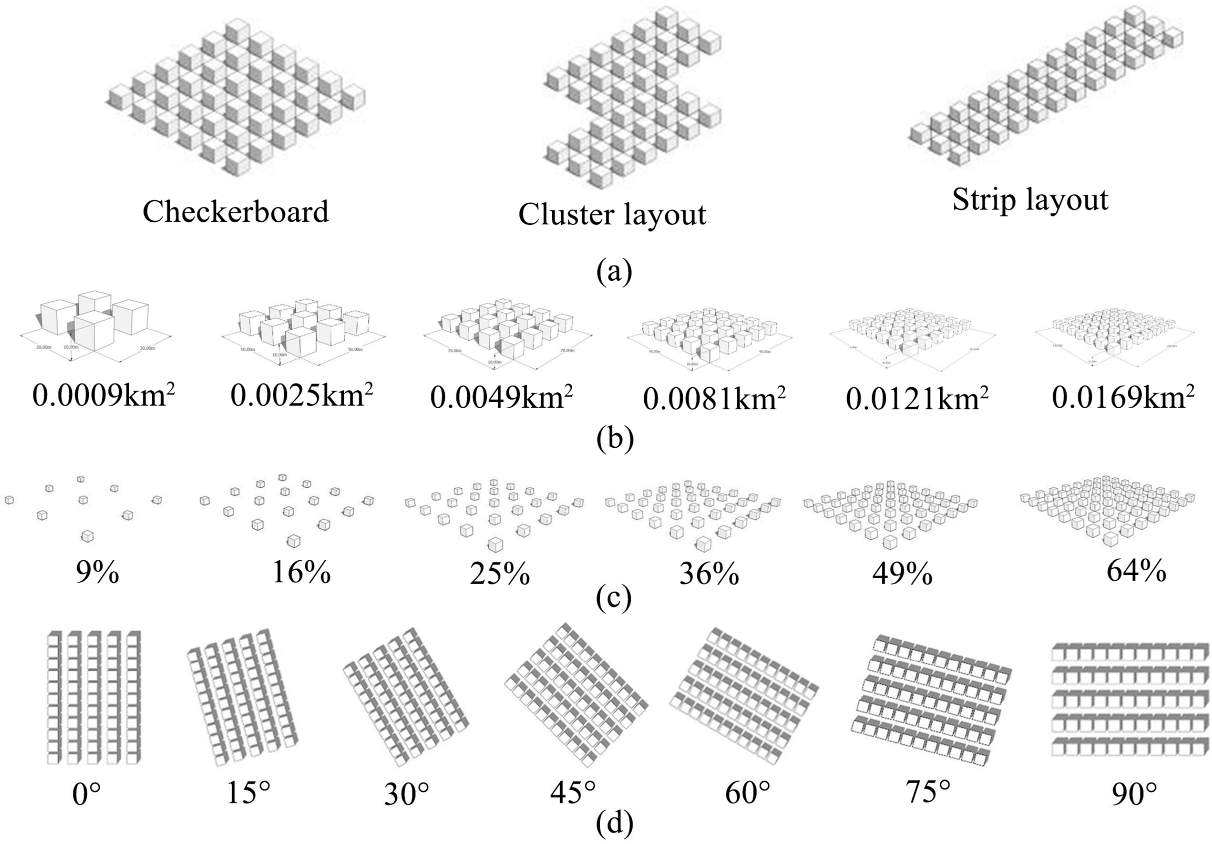

Figure 7. Comparison of spatial morphological indicators of villages. (**a**) Differences in planar morphology; (**b**) differences in scale; (**c**) differences in building density; (**d**) differences in village orientation.

3. Results and Discussion

The previous text has established a wind environment evaluation system for coastal villages on Naozhou Island and verified the feasibility of the software simulation method. The average wind speed, wind speed amplification factor, and wind field coefficients K1 and K2 have been identified as key evaluation indicators. Four sets of models have been established to explore the relationship between different village spatial forms and the wind environment. On this basis, this chapter will discuss the simulation experiment results, analyzing the specific impacts of different spatial form variables (plan form, village scale, building density, village orientation) on the village wind field under normal and extreme wind conditions, aiming to reveal the intrinsic connection between village morphology and wind field changes, providing a scientific basis for subsequent optimization.

3.1. The Impact of Village Spatial Morphology on Wind Environment

Figure 8 shows the wind speed cloud maps of different village forms under two wind conditions, including the simulation results of average wind speed, wind speed amplification factor, and wind field coefficient K1.

From Figure 8, it can be seen that under normal wind conditions (a southeast wind, with a wind speed of 2.57 m/s), the average wind speed in the village is influenced by its layout, with the checkerboard layout having an average wind speed of 2.34 m/s, followed by the strip layout at 2.19 m/s, and the clustered layout at 2.02 m/s. The wind speed amplification factor, however, is relatively unaffected by the village's planar morphology, with all three models having a wind speed amplification factor around 1. As the village morphology changes from a checkerboard layout to a clustered layout, the wind field coefficient decreases from 10.8 to 9.24, demonstrating that the checkerboard layout is optimal for wind field comfort. A comparison of the three indicators indicates that the checkerboard layout allows people to feel more comfortable. In extreme wind conditions (an east wind, with a wind speed of 21.70 m/s), the wind speed amplification factor for the strip layout is lower than that of the other two layouts, indicating it is optimal for wind field stability, while, in terms of wind field safety, the order is strip layout > clustered layout > checkerboard layout. In summary, it can be concluded that, under normal summer wind conditions, the checkerboard layout creates a better wind environment, making it easier for individuals to feel comfortable, and demonstrates good adaptability to the wind environment on the island. In extreme wind conditions, if the construction of the village aims for wind field safety, the strip layout should be chosen.

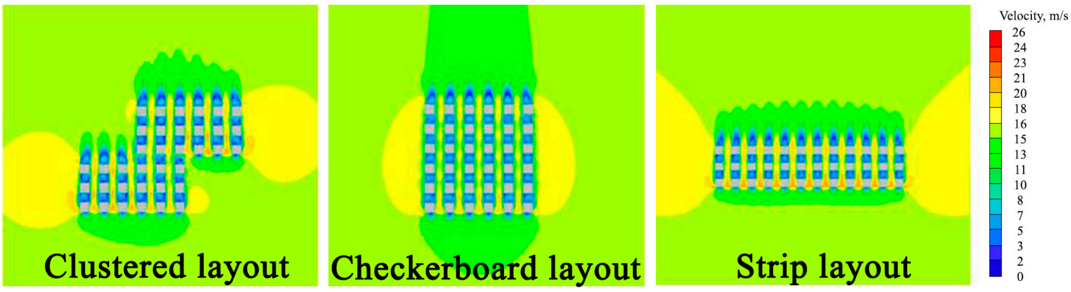

(**a**)

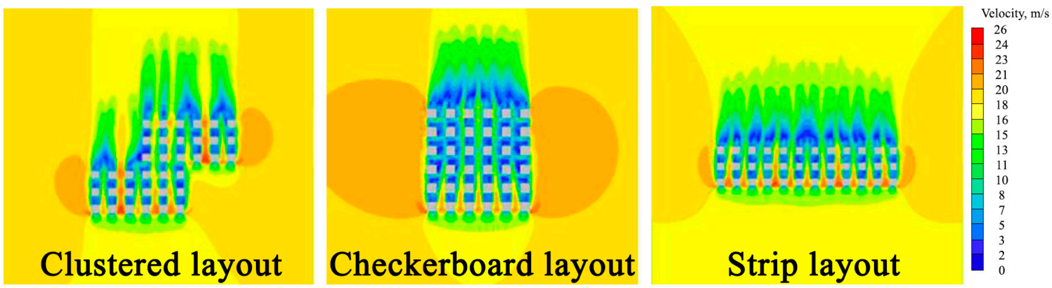

(**b**)

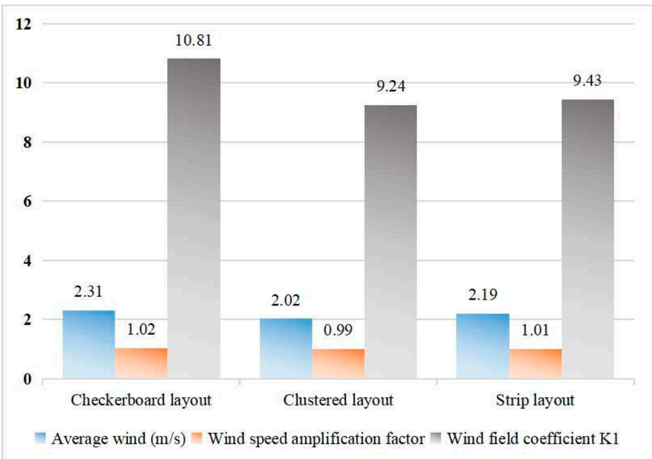

(**c**)

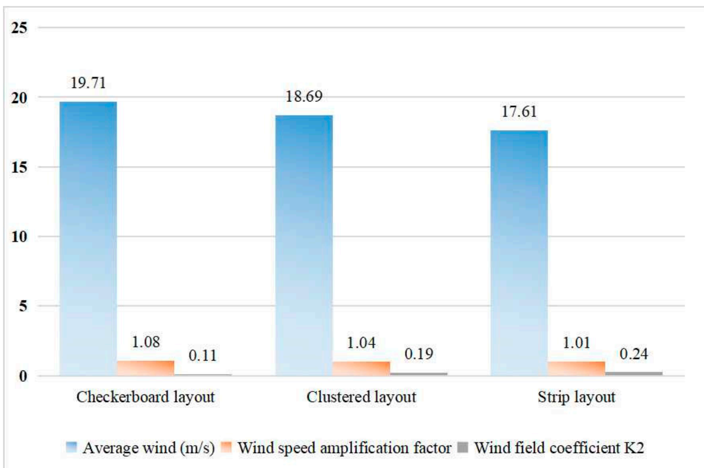

(**d**)

Figure 8. Wind speed cloud maps and simulation values of different village forms under two wind conditions: (**a**,**c**) normal wind conditions; (**b**,**d**) extreme wind conditions.

3.2. Impact of Village Orientation on the Wind Environment

The orientation of the village primarily affects the angle of incidence of the wind. In this subsection of the experiment, under a south wind condition with a wind speed of 10 m/s, the wind environment of villages with different orientations is simulated. In the model setup, the village size is maintained at 11,700 square meters, with the number of buildings kept constant at 55, arranged in 5 columns and 11 rows, with a spacing of 10 m between columns and 2 m between rows, only changing the orientation of the model (Figure 9).

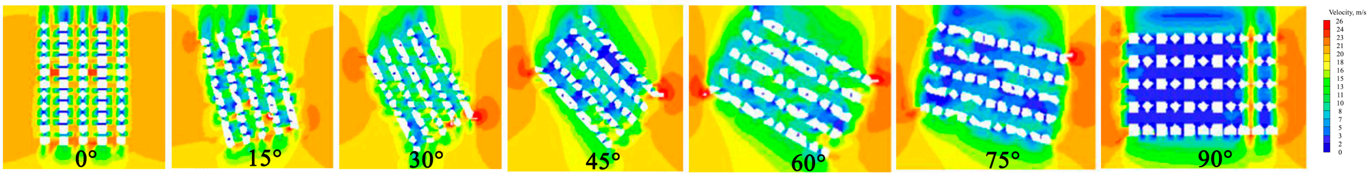

(**a**)

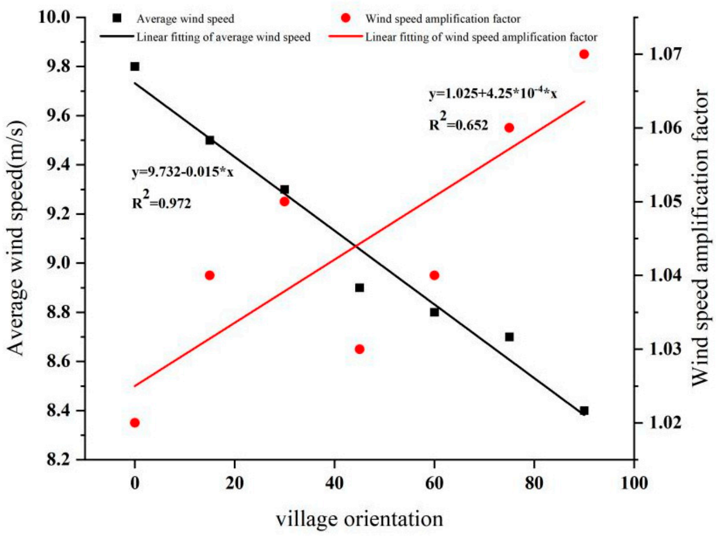

(**b**)

Figure 9. Numerical simulation of different building orientations. (**a**) Village wind speed cloud map; (**b**) simulation data.

By simulating the wind environment of villages with different orientations (Figure 9), and statistically analyzing the simulation results (Table A2), it can be observed that the orientation of the village primarily affects the angle at which wind enters the village. Between 0° and 90°, the angle between the village and the wind direction is inversely proportional to the average wind speed (regression coefficient of −0.015), with a correlation coefficient R^2 of 0.95. This indicates that the smaller the angle between the village and the wind direction, the greater the wind speed. Under normal wind conditions, the wind field is more comfortable, while under extreme wind conditions, the wind field is more dangerous. The stability of the wind field is not significantly correlated with changes in angle (regression coefficient of only 0.0064). In summary, the authors suggest that under normal wind conditions, the orientation of the village should be aligned as closely as possible with the prevailing wind direction to achieve better ventilation benefits. Under extreme wind conditions, it is advisable to avoid alignment with the prevailing wind direction and to form a certain angle to create a larger windward area, thereby resisting strong winds and enhancing the safety of the village's wind field.

3.3. The Impact of Village Scale on Wind Environment

Figure 10 shows the wind speed cloud map for different village sizes, providing the trend and fitting degree of changes in average wind speed, wind speed amplification factor, and wind field coefficient with variations in village size.

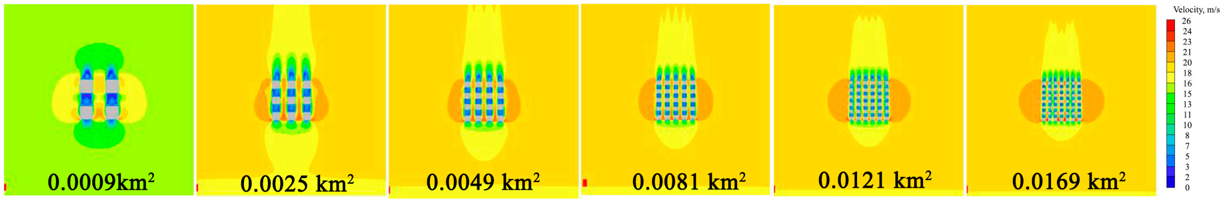

(**a**)

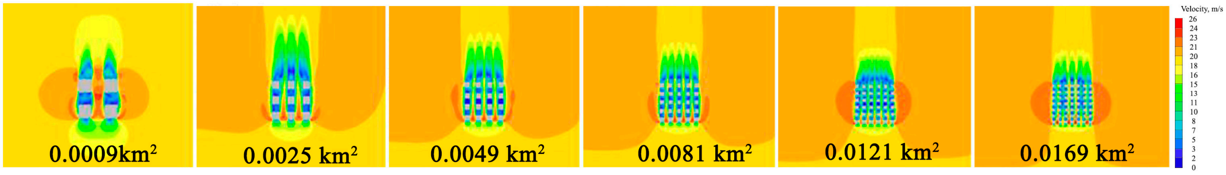

(**b**)

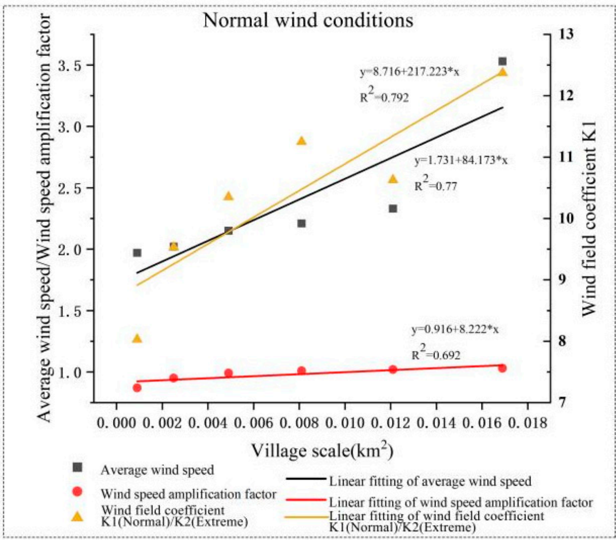

(**c**)

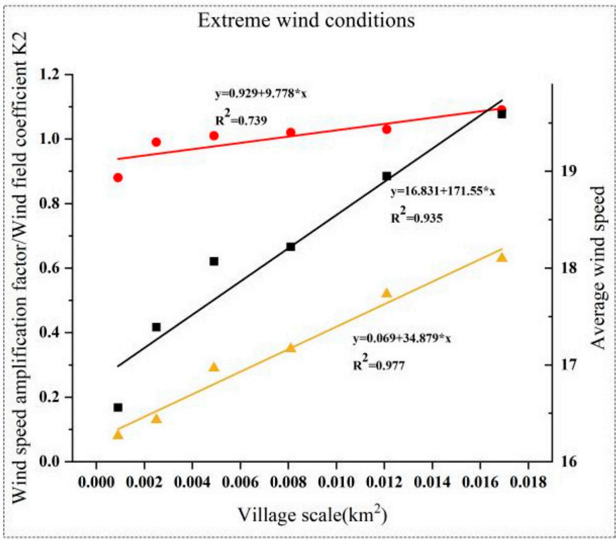

(**d**)

Figure 10. Wind speed cloud maps and simulation values for different village scales under two wind conditions: (**a**,**c**) normal wind conditions; (**b**,**d**) extreme wind conditions.

By simulating the wind environment of villages of different scales, and statistically analyzing the simulation results (Table A2), it can be observed that under both normal wind conditions (a southeast wind, with a wind speed of 2.57 m/s) and extreme wind conditions (an east wind, with a wind speed of 21.70 m/s), the three evaluation indicators are proportional to the village scale within the range of 0.03 km^2 to 0.26 km^2, with correlation coefficients R^2 greater than 0.67. The research results indicate that the village scale has significant explanatory power for the three indicators, particularly for the average wind speed, where the R^2 values for both wind conditions are significantly higher than those for the other two indicators. This clearly indicates a strong correlation between the village scale and the average wind speed, meaning that, as the village scale increases, the average wind speed also increases. Although the village scale also shows a positive correlation with the wind speed amplification factor, its impact is relatively limited. As the village scale continues to expand, the maximum wind speed at a height of 1.5 m above the ground around buildings will also increase. The changes in the wind field coefficients indicate that under normal wind conditions, as the village scale expands, the average wind speed rises, and the comfortable zone is significantly larger than the calm wind zone. Under extreme wind conditions, as the scale increases, the wind field becomes relatively safer. In summary, it can be inferred that the impact of the village scale on the wind environment is significant. Under normal wind conditions, larger village scales correspond to higher average wind speeds and a more comfortable wind field, resulting in a higher overall comfort level of the village's wind field. Under extreme wind conditions, larger villages exhibit a stronger resistance to strong winds.

3.4. The Impact of Building Density on Wind Environment

In the model setup, the village size remains constant at 10,000 square meters, with only the building density being altered. Figure 11 shows the wind speed cloud maps for different village densities, along with the trends and fitting degrees of changes in average wind speed, wind speed amplification factor, and wind field coefficient with variations in village density.

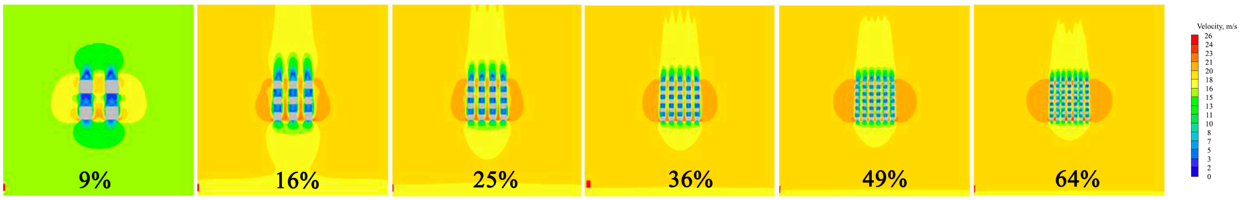

(**a**)

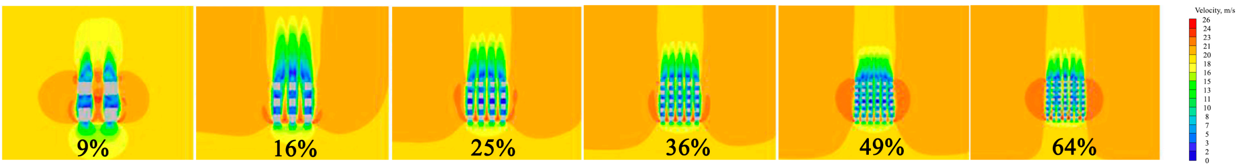

(**b**)

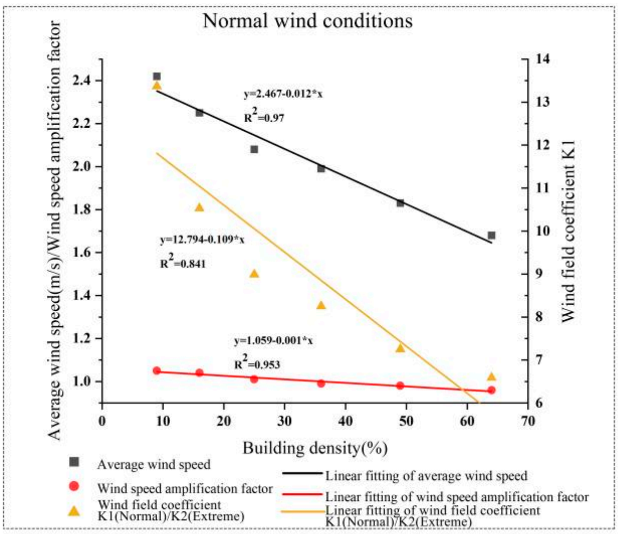

(**c**)

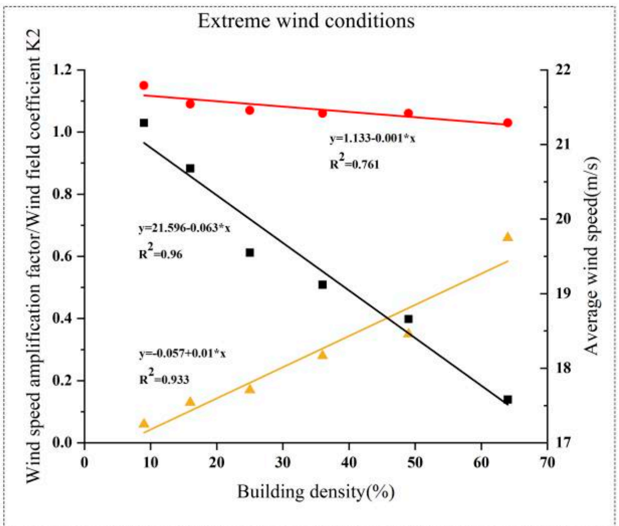

(**d**)

Figure 11. Wind speed cloud maps and simulation values for different building densities under two wind conditions: (**a**,**c**) normal wind conditions; (**b**,**d**) extreme wind conditions.

From the simulation data of two wind conditions (Table A2), it can be observed that the variation in building density has a high explanatory power for the variation of the three dependent variables under both wind conditions. The difference lies in that, under normal wind conditions, building density shows an inverse relationship with average wind speed, wind speed amplification factor, and wind constant K1 (regression coefficients of −0.012, −0.001, and −0.109, respectively). In contrast, under extreme wind conditions, building density exhibits a direct relationship with the wind field coefficient (regression coefficient of 0.01), meaning that the greater the village building density, the safer the wind field. From the wind speed cloud map, it can be seen that when a typhoon approaches, the outdoor wind far exceeds the comfortable range perceived by the human body, and an increase in density helps to block more wind, thereby creating more wind shadow areas. If people stay in this area, they will be relatively safer. Therefore, it can be inferred that, whether under normal or extreme wind conditions, changes in village building density can effectively alter the wind environment.

The above preliminary discussion on the correlation between spatial morphological indicators describing villages and the wind environment at pedestrian height indicates that different spatial forms have varying impacts on the comfort level of pedestrians in villages. Under normal wind conditions, the wind speed in a grid layout can reach 2.34 m/s, which is more suitable for island environments compared with the other two layouts. The density of the village is inversely related to the overall wind environment, while the scale of the village is directly proportional to the overall wind environment. Villages oriented towards the prevailing wind direction will experience higher wind speeds, thereby enhancing comfort within the village. In extreme cases, a strip layout (with a wind speed amplification factor of 1.01) can significantly reduce the hazards posed by typhoons, and villages with high density and large scale can better withstand extreme conditions, creating a larger safe area. In terms of village orientation, it is advisable to avoid alignment with the prevailing wind direction. However, these analyses only consider single factors; in reality, the changes in the wind environment of a village are influenced by multiple factors. Therefore, the following sections will conduct a coupled analysis of various selected spatial forms and wind environments, exploring the correlation and impact degree of each morphological indicator on the wind environment.

3.5. Coupling of Wind Environment and Spatial Form in Village Units

The previous text discussed the changes in a single indicator and environmental indicators, but the wind adaptability of coastal villages on Naozhou Island may not be influenced by a single variable but rather by the combined effects of multiple variables. This section conducts wind environment simulations for the 27 selected villages based on field research data, using SPSS (27) software to analyze the wind environment parameters at pedestrian height in coastal villages and the spatial morphology indicators, distinguishing between those spatial morphologies that have a significant impact on wind environment indicators and those that do not. The planar morphology is a categorical variable (discrete classified category), while the other three morphological indicators are continuous variables (capable of taking continuous values), which are fundamentally different in measurement scale. The mixed use of these may lead to results that are difficult to interpret or even misleading. To ensure the accuracy and interpretability of the analysis results, the following text will only conduct correlation and regression analysis on the three continuous morphological indicators and the four wind environment indicators.

The Pearson matrix in Figure 12 shows the correlation between different morphological indicators and wind environment indicators.

- In two wind conditions, the building density has a strong negative correlation with the average wind speed (extreme wind conditions) and wind speed amplification factor (normal), and there is a weak relationship with the average wind speed (normal) and wind constant coefficient K2, while there is almost no linear relationship with the wind speed amplification factor (extreme).

- In both wind conditions, the village scale has a strong positive correlation with other wind environment indicators, other than having a weak relationship with the average wind speed (extreme).
- In this study, there is no significant relationship between village orientation and wind environment indicators.

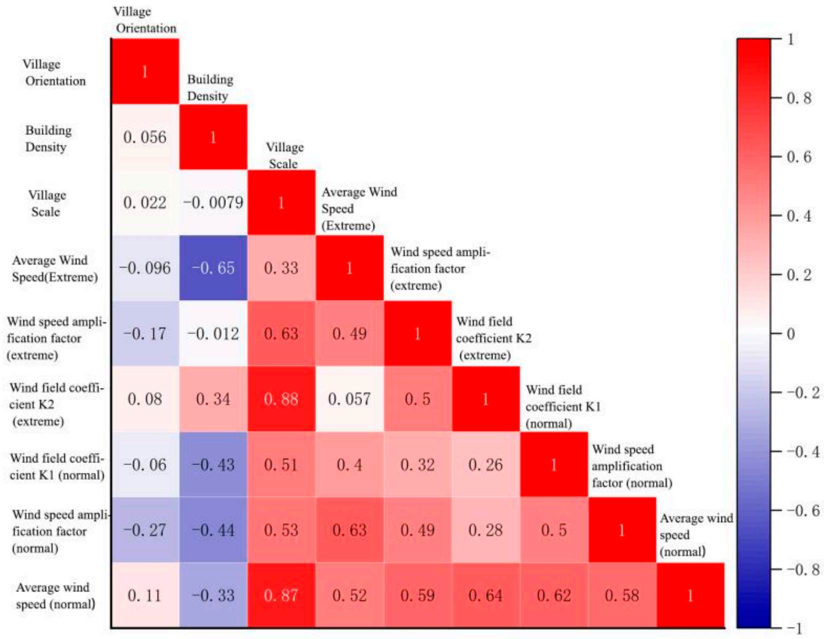

Figure 12. Pearson analysis of morphological and environmental indicators.

According to the results of the Pearson correlation analysis, both building density and village scale have a significant correlation with wind environment indicators, while village orientation shows no obvious relationship with wind environment indicators. This may be due to the complex process of wind field formation, which requires the consideration of multiple linear regression modeling in future research. The following text uses building density, village scale, and village orientation as independent variables in the model to predict the corresponding wind environment effects of a certain pattern.

The fitting of the multiple linear regression is presented in Table A3. A larger R^2 value indicates a better model fit. The constant in the table represents the value of the dependent variable when the independent variable is zero. The regression coefficients are also subjected to hypothesis testing, with corresponding significance provided; it is generally considered significant if the significance is less than or equal to 0.05. Tolerance > 0.1, VIF < 5. There is no multicollinearity in this study.

The regression equation is as follows:

Normal wind conditions:

$$Y_1 = 1.903 + 9.819A_1 - 0.043B_1 + 0.001C_1 \tag{5}$$

$$Y_2 = 1.118 + 0.858A_2 - 0.008B_2 - 3.19 \times 10^{-4}C_2 \tag{6}$$

$$Y_3 = 12.047 + 18.341A_3 - 0.171B_3 - 0.001C_3 \tag{7}$$

Extreme wind conditions:

$$Y_1 = 16.895 + 5.045A_1 - 0.112B_1 + 0.001C_1 \tag{8}$$

$$Y_2 = 1.053 + 0.814A_2 - 0.008B_2 + 4.63 \times 10^{-5}C_2 \tag{9}$$

$$Y_3 = -0.061 + 1.328A_3 + 0.006B_3 - 4.80 \times 10^{-5}C_3 \tag{10}$$

In the formula: Y_1, Y_2, Y_3—represent the average wind speed, wind speed amplification factor, and wind field coefficients K1 (normal)/K2 (extreme); A, B, C represent village scale, village density, and village orientation, respectively.

Through Figure 13, the changes in the goodness of fit and the significance of influencing factors for the two wind condition models can be visually observed. Under normal wind conditions, the R^2 values of the mathematical models are 0.867, 0.545, and 0.449, respectively. Among the three models, the R^2 value for average wind speed is the highest, indicating a high explanatory power for the independent variable, effectively explaining the positive correlation between village scale and average wind speed (regression coefficient of 9.819), meaning that, as the village scale increases, the overall wind comfort of the village also increases, and the negative correlation with building density (regression coefficient of −0.043), indicating that as the village density increases, the overall wind comfort of the village correspondingly decreases. The wind speed amplification coefficient and wind field coefficient K1 have a medium to high explanatory power for the independent variable. In terms of significance, the significance of village orientation is higher than that of other morphological indicators, thus the impact of village orientation on the wind environment is relatively small, and the wind environment indicators can be accurately described by Equations (5)–(7). Under extreme wind conditions, the R^2 values of the mathematical models are 0.538, 0.428, and 0.891, respectively. The R^2 value of the wind field coefficient K2 is the highest, which can better explain its correlation with the village scale and the building density (regression coefficients of −0.061 and 0.006). Meanwhile, the average wind speed and wind speed amplification coefficient have a medium to high explanatory power for the independent variable. From a significance perspective, in the average wind speed and wind field coefficient K2 model, village orientation shows higher significance compared with other morphological indicators. In the wind speed amplification coefficient model, the significance of village orientation and building density exceeds that of the village scale, indicating a relatively strong correlation between the village scale and the wind speed amplification coefficient, the wind environment indicators can be accurately described by Equations (8)–(10).

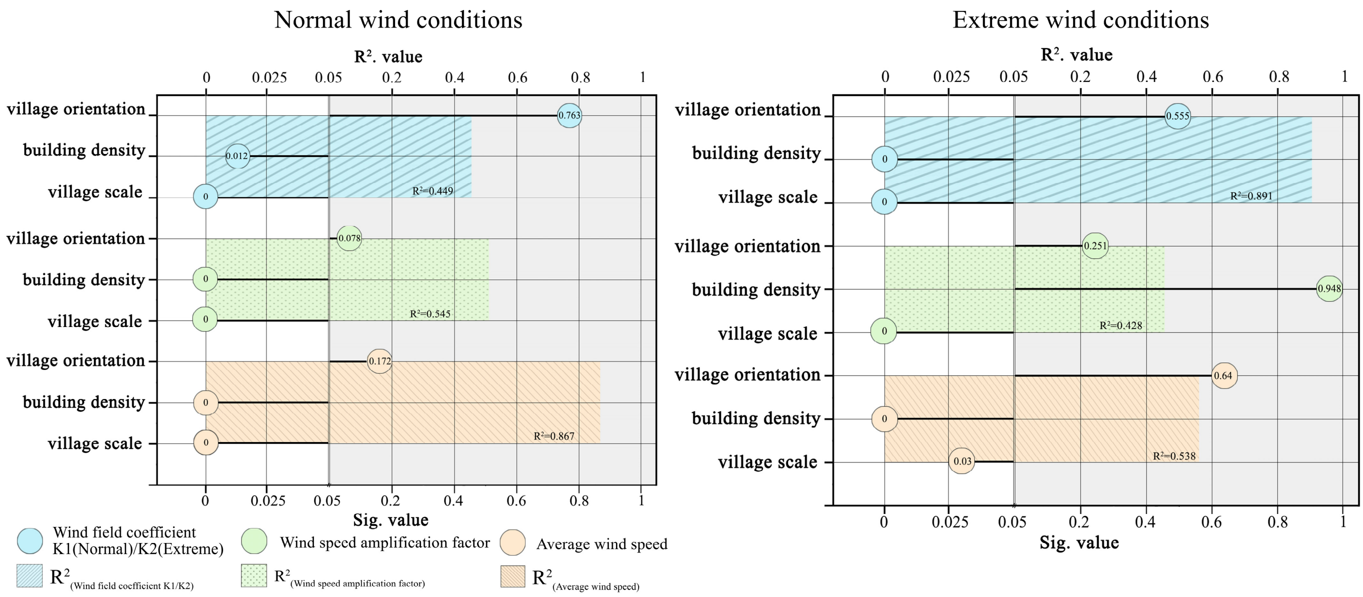

Figure 13. Significance test of village spatial morphology and wind environment indicators under two wind conditions.

In the model, the orientation of the village and the dependent variable showed no significant correlation ($p > 0.05$). Although it can have some impact on wind speed, this variable cannot yield accurate predictive values in the formula. The reason for this result may be the irregular spatial distribution of island villages, where the main orientation is usually closely linked to the direction of the streets. Due to the complexity of the island terrain and the possible lack of unified planning in early construction, the street system is relatively chaotic, characterized by winding paths and variable directions. This irregular street layout further affects the construction of houses within the village, leading to an uneven arrangement of houses, which exacerbates the discontinuity and disorder of the street system. Therefore, in terms of the impact on the wind environment, the orientation of the village does not demonstrate a significant correlation.

Due to the differences in the magnitude and units of the original variables, the regression coefficients of each variable in the formula cannot reflect the differences in the degree of influence. Instead, judgments should be made based on the standardized coefficients, where the sign of the standardized coefficient (positive or negative) indicates the vector relationship between the independent and dependent variables. As shown in Table 4, under normal wind conditions, the negative impact of the building density on the dependent variable is less than the positive impact of the village scale, which is most evident in the variable of average wind speed. In extreme wind conditions, the highest contribution to average wind speed comes from the building density (contribution rate: −62.12%), while the highest contributions to the wind speed amplification factor and wind field coefficient K2 come from the village scale (contribution rates: 76.97%, 69.73%).

Table 4. Table of relative contribution rates.

Wind Conditions	Dependent Variable / Independent Variable	Average Wind Speed	Wind Speed Amplification Factor	Wind Field Coefficient K1	Wind Field Coefficient K2
Normal wind condition	Village Scale	66.10%	43.93%	51.98%	-
	Building Density	−25.67%	−34.75%	−43.23%	-
	Village Orientation	8.22%	−21.31%	−4.78%	-
Extreme wind conditions	Village Scale	31.44%	76.97%	-	69.73%
	Building Density	−62.12%	0.36%	-	27.02%
	Village Orientation	−6.42%	−22.65%	-	3.24%

Relative contribution rate = standardized coefficient of the independent variable/sum of the absolute values of all standardized coefficients of the independent variables.

These three models consist of indicator coefficients and equation constants. Villages with different spatial morphological characteristics will exhibit variations in the types and degrees of wind environment influencing factors, leading to different corresponding regression models. This model is applicable to villages with a scale ranging from 36,500 m^2 to 260,300 m^2, a village density between 9.95% and 30.99%, and an orientation within the range of 70° to 248°. It can serve as an effective tool for assessing the wind environment under normal wind conditions in coastal villages, combined with outdoor wind environment evaluation standards, for wind environment assessment or optimization, aiming to enhance outdoor wind environment comfort. The minimum standard for critical wind speed to meet comfort requirements is established, and through the model, suitable values for the spatial morphological parameters of coastal villages can be inferred, assisting in the formulation of guidelines for village design or renovation and overall morphological optimization.

4. Conclusions

This study takes the coastal village of Naozhou Island in western Guangdong as a case study. First, spatial morphological data were obtained through field surveys. Secondly, the existing policies and standards related to outdoor wind environment evaluation, along with commonly used outdoor wind environment evaluation methods, were analyzed and studied. Based on the research object of this paper, an outdoor wind environment evaluation system for island villages was constructed. Subsequently, numerical simulation software was used to simulate and compare the results with measured data, exploring the relationship between the spatial morphology of island villages and wind adaptability.

The research results indicate that, under normal wind conditions, the layout patterns of villages show a trend of optimal chessboard arrangement, followed by banded arrangement, and relatively weaker group arrangement in terms of adaptability to the wind environment; under extreme wind conditions, the banded layout demonstrates better stability and safety of the wind field. Additionally, we found that spatial morphological indicators such as village scale, building density, and village orientation significantly affect the wind environment. Under normal wind conditions, the contribution rates of village scale to average wind speed, wind speed amplification factor, and wind field coefficient (66.10%, 43.93%, 51.98%) significantly exceed those of village density (−25.67%, −34.75%, −43.23%), highlighting the dominant role of the village scale in optimizing the wind environment.

Based on an in-depth exploration of the relationship between spatial morphology and wind environment, this study reveals the optimization strategies for village layout under different wind conditions. Under normal wind conditions, appropriately expanding the spatial scale of the village helps to improve the quality of the wind environment. Under extreme wind conditions, moderately increasing building density and adopting relatively small-scale village layouts become effective means to enhance the safety of the wind environment. Among these, increasing building density is the more effective method. These principles not only provide a solid scientific basis for the planning and wind environment optimization of island villages but also lay a strong foundation for guiding the sustainable development of island villages and improving the quality of life and safety of the villagers.

However, despite this study employing quantitative analysis methods to explore the climate adaptability patterns of the coastal village layout on Naozhou Island, there are still some limitations:

- The building materials of coastal villages (such as shell waste, granite blocks, and adobe) differ from those in inland areas, which is crucial for wind adaptability and structural resilience. However, this study focuses solely on the impact of spatial morphology on the wind environment and does not delve into the role of building materials. This limits our understanding of the overall adaptability of the village. Future research could explore the performance of building materials in coastal villages within wind environments, revealing their relationship with wind adaptability. Additionally, by enhancing the monitoring of coastal village buildings [39] and employing image processing technology [40], we can gain a clearer understanding of the damage caused by extreme weather and timely develop corresponding solutions.
- In the research process, we focused on investigating whether various independent spatial morphological factors (such as building density, orientation, village orientation, and planar morphology) have a significant effect on the wind environment. This allowed us to deeply analyze the unique contributions of each factor in influencing wind behavior. However, it also led to our failure to explore the potential interactions between spatial morphological indicators and their comprehensive impact on the wind environment. Such interactions may produce wind behavior patterns that differ from expectations, but incorporating them into the research scope would complicate the analysis process, potentially hindering our ability to clearly identify the significant effects of each independent factor on the wind environment. Therefore, in future research, it is necessary to design more complex experiments and simulations to explore the actual impact of these variable combinations on the wind environment.

Author Contributions: Conceptualization, P.X.; methodology, P.X.; software, Z.L. and P.X.; validation, Z.L. and P.X.; investigation, Y.P.; resources, Y.P.; data curation, Z.L.; writing—original draft preparation, Z.L. and L.L.; visualization, Z.L. All authors have read and agreed to the published version of the manuscript.

Funding: This research received no external funding.

Data Availability Statement: The experimental data used to support the findings of this study are included in the article.

Conflicts of Interest: Author Peisheng Xie is employed by the Guangdong Provincial Architectural Design Research Institute Group Co., Ltd. The remaining authors declare that the research was conducted in the absence of any commercial or financial relationships that could be construed as a potential conflict of interest.

Appendix A

Table A1. Table of research on Naozhou Island villages.

	Categorization	Quantities	Proportions	Village Name
Village pattern	Checkerboard layout	16	38.1%	Yingming Village Cunliang Village Jialixin Village Dawen Village Danshui Village Doulong Village Houjiao Village Chima Village Songhuang Village Mengxi Village Naganwei Village Nafan Village Tantanzai Village Tantan Village Yanlou Village Nakunzai Village.
	Cluster Layout	16	38.1%	Zhouwu Village, Zhucai Village, Yanting Village, Liuzhu Village, Nakun Village, Beizhai Village, Yingfan Village, Jialiu Old Village, Tianxuan Village, Tanbeihu Village, Zhengpeng Village, Naguang Village, Mengdong Village, Dalinhou Village, Xianadong Village, Dingdang Village.
	Strip layout	9	21.4%	Longchi Village, Nangang Village, Xibu Village, Honggong Village, Dalang Village, Beijin Village, Xundizai Village, Liangwu Village, Liuluo Village
	Distributed layout	1	2.3%	Gangtou Village
	(grand) Total	42	100%	
Village size	Micro-village	3	7.1%	Yingfan Village, Tantan Village, Dingdang Village.
	Small village	16	38.0%	Zhouwu Village, Yingming Village, Dawen Village, Danshui Village, Houjiao Village, Yanting Village, Liuzhu Village, Mengxi Village, Naganwei Village, Tantanzai Village, Jialiu Old Village, Gangtou Village, Zhengpeng Village, Nakunzai Village, Xianadong Village, Liuluo Village.
	Medium-sized villages	13	31.0%	Jialixin Village, Honggong Village, Doulong Village, Beijin Village, Chima Village, Songhuang Village, Nakun Village, Beizhai Village, Longchi Village, Xibu Village, Liangwu Village, Nafan Village, Naguang Village.
	Large villages	7	16.7%	Cunliang Village, Dalang Village, Nangang Village, Xundizai Village, Tanbeihu Village, Yanlou Village, Dalinhou Village.
	Mega-village	3	7.1%	Zhucai Village, Tianxuan Village, Mengdong Village.
	(grand) total	42	100%	
Village orientation	lit. sit north, face south (idiom); figure facing south	12	28.6%	Yingming Village, Xibu Village, Honggong Village, Danshui Village, Chima Village, Mengxi Village, Nafan Village, Tantanzai Village, Nakunzai Village, Liuzhu Village, Mengdong Village, Dingdang Village, Nakun Village, Beizhai Village, Yanting Village, Liuluo Village.
	sit northeast to face southwest	4	9.5%	NaKun Village, BeiZhai Village, YanTing Village, LiuLuo Village,
	lit. sitting northwest, facing southeast	12	28.6%	Jialixin Village, Cunliang Village, Dawen Village, Songhuang Village, Zhouwu Village, Zhucai Village, Tanbeihu Village, Yingfan Village, Jialiu Old Village, Tianxuan Village, Xianadong Village, Nangang Village.

Table A1. *Cont.*

	Categorization	Quantities	Proportions	Village Name
Village orientation	sit south and face north	3	7.1%	Doulong Village, YanLou Village, NaGuang Village
	sit southeast, face northwest	4	9.5%	Dalang Village, Houjiao Village, Tantan Village, Gangtou Village.
	sit southwest to face northeast	1	2.4%	LiangWu Village
	sit east and face west	3	7.1%	Beijin Village, Naganwei Village, Xundizai Village.
	sit west and face east	1	2.4%	Longchi Village
	no specific orientation	2	4.7%	Zhengpeng Village, Dalinhou Village.
	(grand) Total	42	100%	
Village density	less than 10%	2	5%	Mengdong Village, Xianadong Village
	10–20%	16	38%	Honggong Village, Dawen Village, Dalang Village, Beijin Village, Xundizai Village, Nafan Village, Tantanzai Village, Tantan Village, Zhucai Village, Yingfan Village, Jialiu Old Village, Naguang Village, Dalinhou Village, Liuluo Village, Longchi Village, Gangtou Village
	20–30%	21	50%	Yingming Village, Cunliang Village, Jialixin Village, Danshui Village, Doulong Village, Houjiao Village, Songhuang Village, Mengxi Village, Naganwei Village, Yanlou Village, Nakunzai Village, Yanting Village, Liuzhu Village, Nakun Village, Beizhai Village, Liangwu Village, Tianxuan Village, Tanbeihu Village, Zengpeng Village, Nangang Village, Xibu Village
	30–40%	2	5%	Chima Village, Zhouwu Village
	40% or more	1	2%	Dingdang Village
	(grand) total	42	100%	

Table A2. Measured and software simulated data for villages under normal wind conditions.

Village Name	Village Orientation	Village Size	Building Density	Wind Field Coefficient K1/K2		Wind Speed Amplification Factor		Average Wind Speed(m/s)	
				N	E	N	E	N	E
Liuzhu Village	175°	4.94	20.15	7	0.153	0.913	1.006	1.64	15.03
Yanting Village	230°	6.8	26.77	8.17	0.19	0.86	0.984	2.25	14.31
Zhouwu Village	140°	4.64	30.99	8.35	0.196	0.874	1.068	1.22	13.16
Zhucai Village	135°	22.79	13.71	13.29	0.362	1.237	1.189	4.07	16.54
Yingfan Village	143°	3.65	25.4	7.18	0.168	0.906	1.0887	1.49	14.03
Jialiu Old Village	150°	6.5	15.99	8.17	0.1192	1.067	1.129	1.81	15.12
Tianxuan Village	146°	26.03	27.78	14.19	0.42	1.085	1.38	3.79	14.88
Tanbeihu Village	152°	15.01	20.9	8.93	0.23	0.944	1.148	2.34	15.23
Xianadong Village	120°	4.44	9.95	12.62	0.06	1.008	0.978	2.22	14.68
Yingming Village	185°	6.98	27.24	7.45	0.194	0.877	1.018	1.51	13.16
Tantanzai Village	180°	5.35	16.23	12.23	0.04	1.022	1.105	2.01	15.22
Houjiao Village	300°	5.16	26.61	5.17	0.188	0.76	1.148	1.86	14.3
Tantan Village	310°	3.67	26	10.45	0.175	1.023	1.056	1.37	14.35
Doulong Village	352°	7.69	21.83	12.32	0.186	0.83	0.988	1.9	14.32
Yanlou Village	356°	19.34	21.95	10.25	0.33	1.053	1.138	3.3	15.48

Table A2. *Cont.*

Village Name	Village Orientation	Village Size	Building Density	Wind Field Coefficient K1/K2		Wind Speed Amplification Factor		Average Wind Speed(m/s)	
				N	E	N	E	N	E
Cunliang Village	129°	18.97	27.51	9.4	0.321	1.114	1.068	2.37	14.44
Jialixin Village	127°	7.45	24.25	8.27	0.202	1.027	1.0881	1.6	14.04
Dawen Village	133°	5.81	17.97	11.37	0.138	0.953	1.077	1.75	14.86
Xibu Village	180°	8.92	23.97	9.85	0.21	0.972	1.096	1.49	14.49
Honggong Village	178°	8.35	14.32	9.45	0.15	1.146	1.218	2.23	18.04
Liuluo Village	222°	5.94	17.82	9.74	0.068	0.955	1.0881	1.76	15.27
Beijin Village	273°	7.14	18.36	9.7	0.1142	1.005	1.067	2.22	14.77
Xundizai Village	271°	12.16	10.15	10.09	0.22	1.018	1.088	2.79	15.06
Dalang Village	313°	19.99	18.22	13.49	0.352	0.973	1.128	3.2	15.37
Nangang Village	132°	14.62	20.55	11.28	0.3	0.964	1.106	2.12	15.26
Liangwu Village	42°	8.94	22.8	10.27	0.23	0.965	1.118	1.82	15.32
Longchi Village	90°	8.99	14.09	13.36	0.1082	1.028	1.147	2.65	16.13

N: Normal wind conditions, **E:** Extreme wind conditions.

Table A3. Regression coefficients and their significance tests and multiple covariance tests.

Mold			Unstandardized Coefficient		Standardized Coefficient	T	Significance	Covariance Statistics		R^2	F-Value
			B	Standard Error				Tolerances	VIF		
Normal wind condition	Average wind speed	(Constant)	1.903	0.254		7.482	<0.001			0.867	50.158 ***
		Village size	9.819	0.867	0.86	11.326	<0.001	0.999	1.001		
		Building density	−0.043	0.01	−0.334	−4.389	<0.001	0.997	1.003		
		Village orientation	0.001	0.001	0.107	1.411	0.172	0.996	1.004		
	Wind speed amplification factor	(Constant)	1.118	0.066		16.931	<0.001			0.545	50.158 ***
		Village size	0.858	0.225	0.536	3.81	0.001	0.999	1.001		
		Building density	−0.008	0.003	−0.424	−3.008	0.006	0.997	1.003		
		Village orientation	-3.19×10^{-4}	1.73×10^{-4}	−0.26	−1.841	0.078	0.996	1.004		
	K1	(Constant)	12.047	1.629		7.398	<0.001			0.449	6.252 **
		Village size	18.341	5.552	0.511	3.304	0.003	0.999	1.001		
		Building density	−0.171	0.062	−0.425	−2.743	0.012	0.997	1.003		
		Village orientation	−0.001	0.004	−0.047	−0.305	0.763	0.996	1.004		
Extreme wind conditions	Average wind speed	(Constant)	16.895	0.64		26.392	<0.001			0.538	8.943 ***
		Village size	5.045	2.182	0.328	2.312	0.03	0.999	1.001		
		Building density	−0.112	0.025	−0.648	−4.564	<0.001	0.997	1.003		
		Village orientation	−0.001	0.002	−0.067	−0.473	0.64	0.996	1.004		
	Wind speed amplification factor	(Constant)	1.053	0.06		17.657	<0.001			0.428	5.740 ***
		Village size	0.814	0.203	0.632	4.004	0.001	0.999	1.001		
		Building density	4.63×10^{-5}	0.002	0.003	0.02	0.984	0.997	1.003		
		Village orientation	−0.0001	0.0001	−0.186	−1.177	0.251	0.996	1.004		
	K2	(Constant)	−0.061	0.03		−2.006	0.057			0.891	62.610 ***
		Village size	1.328	0.104	0.88	12.777	<0.001	0.999	1.001		
		Building density	0.006	0.001	0.341	4.937	<0.001	0.997	1.003		
		Village orientation	4.80×10^{-5}	0.00008	0.041	0.599	0.555	0.996	1.004		

** $p < 0.01$, *** $p < 0.001$.

References

1. Yuan, C.; Ng, E.; Norford, L.K. Improving Air Quality in High-Density Cities by Understanding the Relationship between Air Pollutant Dispersion and Urban Morphologies. *Build. Environ.* **2014**, *71*, 245–258. [CrossRef] [PubMed]
2. Guo, A.; Yang, J.; Xiao, X.; Xia, J.; Jin, C.; Li, X. Influences of Urban Spatial Form on Urban Heat Island Effects at the Community Level in China. *Sustain. Cities Soc.* **2020**, *53*, 101972. [CrossRef]

3. Scislo, L.; Szczepanik-Scislo, N. Influence of Mechanical Ventilation and Cooling Systems on Vibrations of High Precision Machines. *E3S Web Conf.* **2019**, *100*, 00080. [CrossRef]
4. Miao, Y.; Chiou, S.-C. Study on the Wind Environment of the Architecture Communities: Traditional Typical Min Nan Human Settlements' Case. *Math. Probl. Eng.* **2013**, *2013*, 467076. [CrossRef]
5. Asfour, O.S. Prediction of Wind Environment in Different Grouping Patterns of Housing Blocks. *Energy Build.* **2010**, *42*, 2061–2069. [CrossRef]
6. Chen, Y. Application of a Wind Environment Simulation Generation Technology in Urban Planning. *Wirel. Commun. Mob. Comput.* **2022**, *2022*, 7939777. [CrossRef]
7. Ji, H.; Li, Y.; Li, J.; Ding, W. A Novel Quantitative Approach to the Spatial Configuration of Urban Streets Based on Local Wind Environment. *Land* **2023**, *12*, 2102. [CrossRef]
8. Kubota, T.; Miura, M.; Tominaga, Y.; Mochida, A. Wind Tunnel Tests on the Relationship between Building Density and Pedestrian-Level Wind Velocity: Development of Guidelines for Realizing Acceptable Wind Environment in Residential Neighborhoods. *Build. Environ.* **2008**, *43*, 1699–1708. [CrossRef]
9. Ma, T.; Chen, T. Outdoor Ventilation Evaluation and Optimization Based on Spatial Morphology Analysis in Macau. *Urban Clim.* **2022**, *46*, 101335. [CrossRef]
10. Takemi, T.; Yoshida, T.; Horiguchi, M.; Vanderbauwhede, W. Large-Eddy-Simulation Analysis of Airflows and Strong Wind Hazards in Urban Areas. *Urban Clim.* **2020**, *32*, 100625. [CrossRef]
11. Zhao, H.; Jiang, X.; Cao, Y.; Zhang, H.; Zhen, S.; Jia, R.; Zhang, S. Wind Environment Simulation and Optimisation Strategies for Block Spatial Forms in Cold Low Mountainous Areas—a Case Study of Changchun, China. *Sustainability* **2022**, *14*, 6643. [CrossRef]
12. Hsieh, C.-M.; Yu, C.-Y.; Shao, L.-Y. Improving the Local Wind Environment through Urban Design Strategies in an Urban Renewal Process to Mitigate Urban Heat Island Effects. *J. Urban Plan. Dev.* **2023**, *149*. [CrossRef]
13. Qi, L.; Liu, R.; Cui, Y.; Zhou, M.; Bonenberg, W.; Song, Z. Study of the Landscape Pattern of Shuiyu Village in Beijing, China: A Comprehensive Analysis of Adaptation to Local Microclimate. *Sustainability* **2021**, *14*, 375. [CrossRef]
14. Shawei, Z.; Zhong, Y.; Dinghang, W.; Jin, T. Landscape Pattern in Traditional Village--Thinking over the Zhonglou Village, Conghua. *Iop Conf. Ser. Earth Environ. Sci.* **2018**, *153*, 052014. [CrossRef]
15. Xu, X.; Genovese, P.V.; Zhao, Y.; Liu, Y.; Woldesemayat, E.M.; Zoure, A.N. Geographical Distribution Characteristics of Ethnic-Minority Villages in Fujian and Their Relationship with Topographic Factors. *Sustainability* **2022**, *14*, 7727. [CrossRef]
16. Chen, J.; Lin, W.; Zhang, Y.; Dai, Y.; Chen, B. Village Fengshui Forests as Forms of Cultural and Ecological Heritage: Interpretations and Conservation Policy Implications from Southern China. *Forests* **2020**, *11*, 1286. [CrossRef]
17. Zhang, D.; Gao, W.; Lv, Y. The Triple Logic and Choice Strategy of Rural Revitalization in the 70 Years since the Founding of the People's Republic of China, Based on the Perspective of Historical Evolution. *Agriculture* **2020**, *10*, 125. [CrossRef]
18. Xu, F.; Gao, Z.; Xing, Y.; Wu, Z.; Zhang, J.; Liao, Y.; Hu, Y. The Effect of Village Morphological Variation Caused by Economic Development on Residents' Health and Rural Ventilation in Tianjin. *Buildings* **2022**, *12*, 1393. [CrossRef]
19. Zang, H.Y.; Hsieh, C.-M.; Cang, Y.; Gu, M. Microclimate Adaptability Analysis of Waterfront Traditional Villages: A Case Study of Mingyuewan Village in Suzhou. *J. Water Clim. Change* **2023**, *14*, 3329–3344. [CrossRef]
20. Xiong, Y.; Zhang, J.; Yan, Y.; Sun, S.; Xu, X.; Higueras, E. Effect of the Spatial Form of Jiangnan Traditional Villages on Microclimate and Human Comfort. *Sustain. Cities Soc.* **2022**, *87*, 104136. [CrossRef]
21. Sun, R.; Dong, J.; Zhao, H.; Wang, L.; Qin, D. Typical Village and Town Houses in the Cold Region of Northeast China: Simulation Analysis of Courtyard Layout and Winter Wind Environment Habitability. *Buildings* **2023**, *14*, 109. [CrossRef]
22. Gou, S.; Li, Z.; Zhao, Q.; Nik, V.M.; Scartezzini, J.-L. Climate Responsive Strategies of Traditional Dwellings Located in an Ancient Village in Hot Summer and Cold Winter Region of China. *Build. Environ.* **2015**, *86*, 151–165. [CrossRef]
23. Guo, J.; Han, G.; Xie, Y.; Cai, Z.; Zhao, Y. Exploring the Relationships between Urban Spatial Form Factors and Land Surface Temperature in Mountainous Area: A Case Study in Chongqing City, China. *Sustain. Cities Soc.* **2020**, *61*, 102286. [CrossRef]
24. He, J.; Chen, Y.; Zheng, L.; Zheng, J. Research on Wind Environment and Morphological Effects of High-Rise Buildings in Macau: An Example from the New Reclamation Area around Areia Preta. *Int. J. Environ. Res. Public Health* **2023**, *20*, 4143. [CrossRef] [PubMed]
25. Du, Z.; Guo, W.; Li, W.; Gao, X. A Study on the Optimization of Wind Environment of Existing Villa Buildings in Lingnan Area: A Case Study of Jiangmen's "Yunshan Poetic" Moon Island Houses. *Buildings* **2022**, *12*, 1304. [CrossRef]
26. Meir, I.A.; Pearlmutter, D.; Etzion, Y. On the Microclimatic Behavior of Two Semi-Enclosed Attached Courtyards in a Hot Dry Region. *Build. Environ.* **1995**, *30*, 563–572. [CrossRef]
27. Liu, K.S.; Chan, J.C.L. Climatological Characteristics and Seasonal Forecasting of Tropical Cyclones Making Landfall along the South China Coast. *Mon. Wea. Rev.* **2003**, *131*, 1650–1662. [CrossRef]
28. Cheng, V.; Ng, E. Thermal Comfort in Urban Open Spaces for Hong Kong. *Archit. Sci. Rev.* **2011**, *49*, 236–242. [CrossRef]
29. *HJ/T 393-2007*; Technical Specifications for Urban Fugitive Dust Pollution Prevention and Control. China Environmental Science Press: Beijing, China, 2007.
30. *ASCE/SEI 49-21*; Standard for Wind Tunnel Test of Buildings and Structures. China Architecture & Building Press: Beijing, China, 2015.

31. *JGJ/T 449-2018*; Standard for Green Performance Calculation of Civil Buildings. Ministry of Housing and Urban-Rural Development of the People's Republic of China: Beijing, China, 2018.
32. Tsang, C.W.; Kwok, K.C.S.; Hitchcock, P.A. Wind Tunnel Study of Pedestrian Level Wind Environment around Tall Buildings: Effects of Building Dimensions, Separation and Podium. *Build. Environ.* **2012**, *49*, 167–181. [CrossRef]
33. Ma, T.; Chen, T. Classification and Pedestrian-Level Wind Environment Assessment among Tianjin's Residential Area Based on Numerical Simulation. *Urban Clim.* **2020**, *34*, 100702. [CrossRef]
34. Toparlar, Y.; Blocken, B.; Maiheu, B.; Van Heijst, G.J.F. A Review on the CFD Analysis of Urban Microclimate. *Renew. Sustain. Energy Rev.* **2017**, *80*, 1613–1640. [CrossRef]
35. Blocken, B. Computational Fluid Dynamics for Urban Physics: Importance, Scales, Possibilities, Limitations and Ten Tips and Tricks towards Accurate and Reliable Simulations. *Build. Environ.* **2015**, *91*, 219–245. [CrossRef]
36. Blocken, B. LES over RANS in Building Simulation for Outdoor and Indoor Applications: A Foregone Conclusion? *Build. Simul.* **2018**, *11*, 821–870. [CrossRef]
37. Yang, L.; Li, Y. Thermal Conditions and Ventilation in an Ideal City Model of Hong Kong. *Energy Build.* **2011**, *43*, 1139–1148. [CrossRef]
38. Wu, S.; Zhang, L.; Han, Z.; Hu, C.; An, D. Research on Microclimate Optimization of Traditional Residential Buildings in Central Anhui Based on Humid and Hot Climate Characteristics and Regional Architectural Features. *Buildings* **2024**, *14*, 2323. [CrossRef]
39. Sun, H.; Burton, H.V.; Huang, H. Machine Learning Applications for Building Structural Design and Performance Assessment: State-of-the-Art Review. *J. Build. Eng.* **2021**, *33*, 101816. [CrossRef]
40. Pimenov, D.Y.; Da Silva, L.R.R.; Ercetin, A.; Der, O.; Mikolajczyk, T.; Giasin, K. State-of-the-Art Review of Applications of Image Processing Techniques for Tool Condition Monitoring on Conventional Machining Processes. *Int. J. Adv. Manuf. Technol.* **2024**, *130*, 57–85. [CrossRef]